運輸省港湾技術研究所 (25th Anniversary Issue)

港湾技術研究所報告

REPORT OF THE PORT AND HARBOUR RESEARCH INSTITUTE

MINISTRY OF TRANSPORT

VOL. 26 NO. 5 DEC. 1987

NAGASE, YOKOSUKA, JAPAN

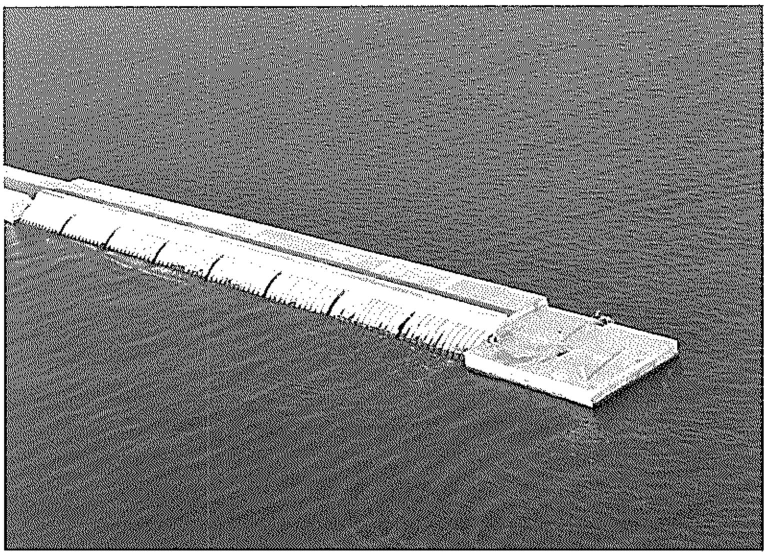

Curved Slit Caisson Breakwater

View of curved slit caisson breakwater completed in the construction at the port of Funakawa. (Courtesy of Akita Port Construction Office, the First District Port Construction Bureau, Ministry of Transport)

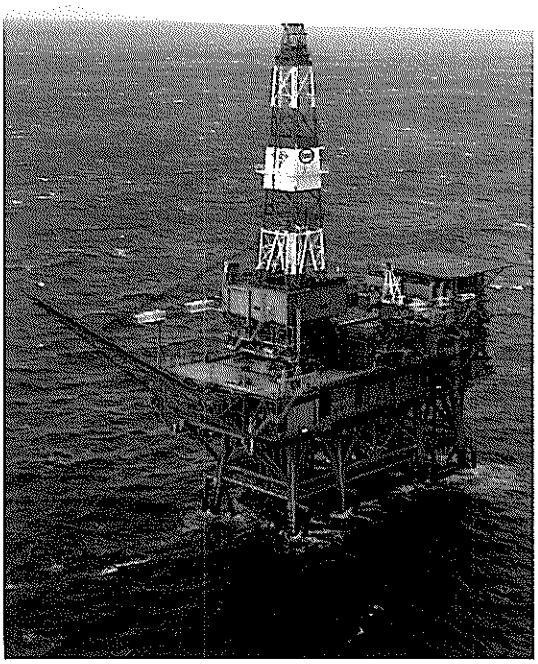

Facilities for Ocean Directional Wave Measurement

Four step type wave gauges and a two-axis directional current meter with a pressure sensor are installed on the legs of an offshore oil rig. They are operated simultaneously for detailed directional wave analysis.

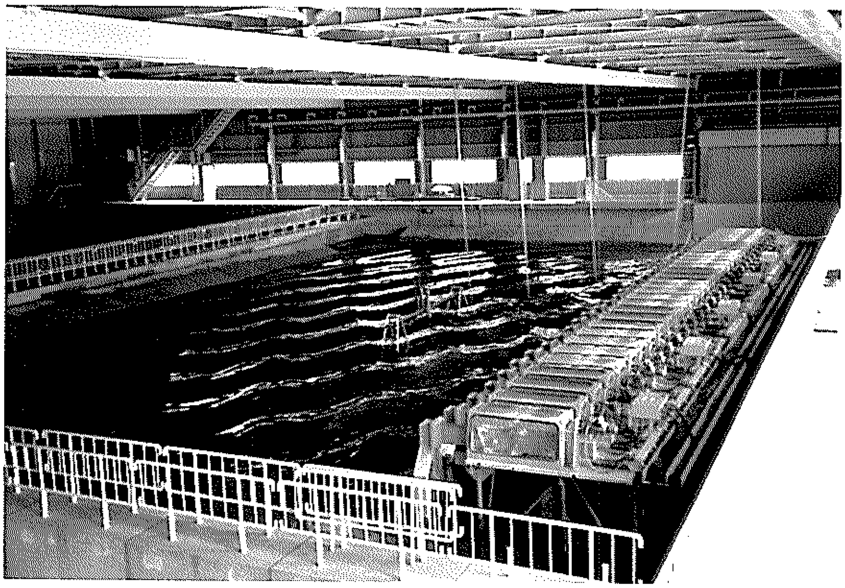

Serpent-type Wave Generator

The photograph shows the serpent-type wave generator in the short-crested wave basin and the superimposition state of two different oblique waves generated by the generator.

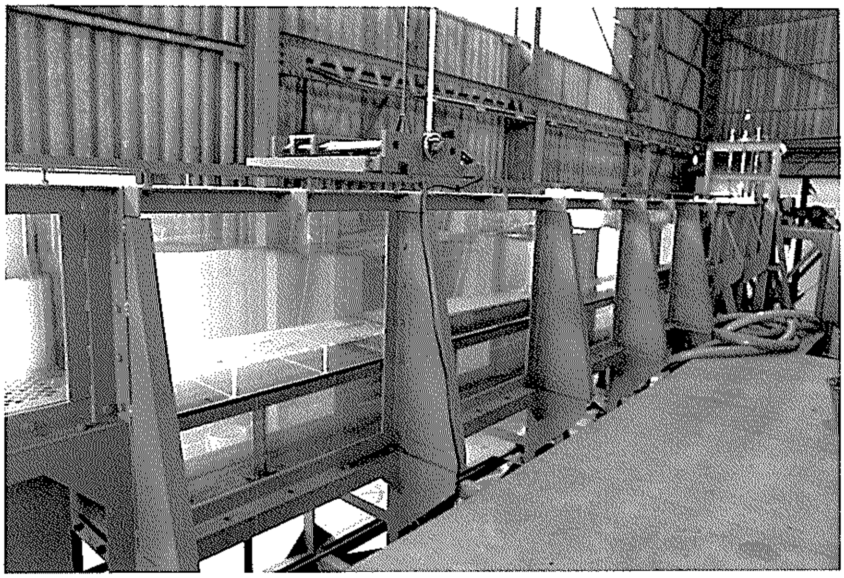

Wave-soil Tank

The experiments concerning the wave-soil interactions are conducted in this tank. The soil tank and the test section are located at the center of the tank. A movable floor is provided at the bottom of the test section and the level of the interface of mud layer and water can easily be adjusted to the level of the flume bottom.

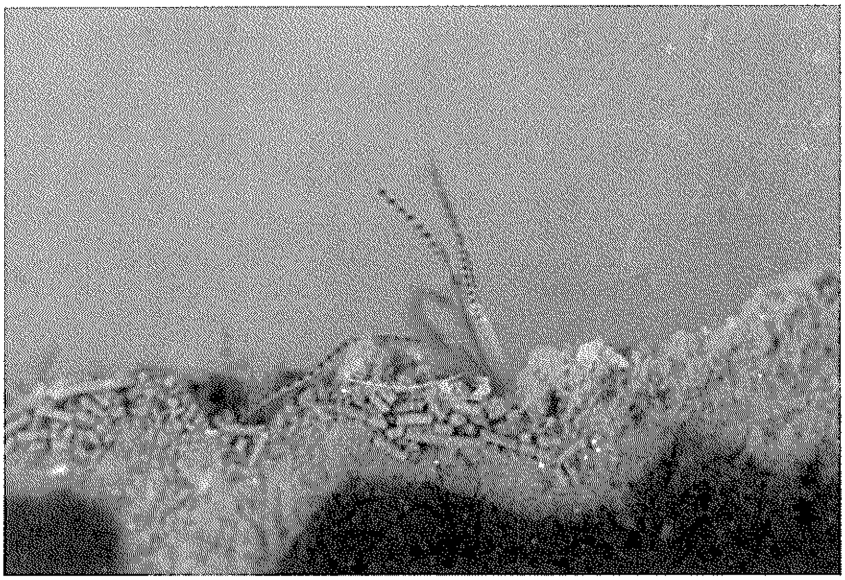

Pararionospio Pinnata

The biomass of benthos is one of the most sensitive indices to know the effect of sea-bed sediment treatments on the marine environmental improvement. The picure shows a kind of benthos, *pararionospio pinnata,* which preferentially exists in the polluted sea-bed.

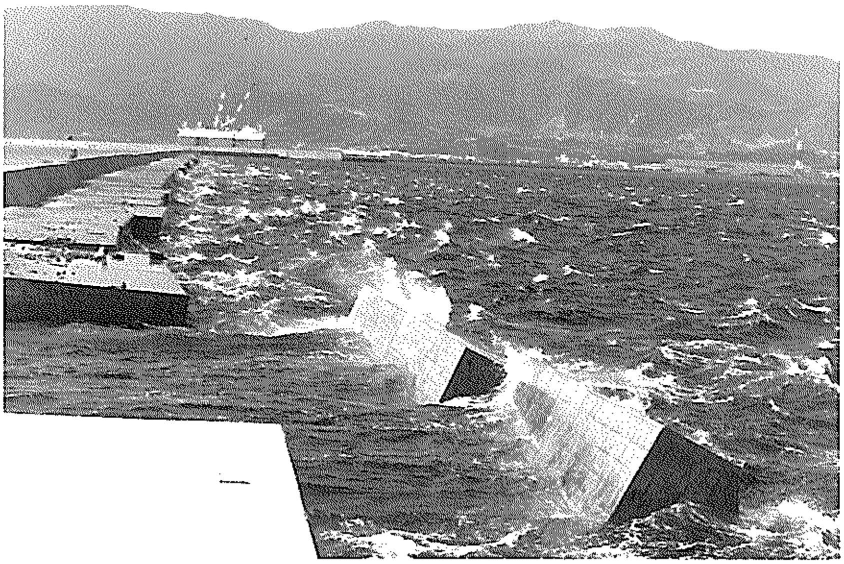

Breakwater Damaged by Storm

This photograph shows a breakwater damage by a storm.
The breakwater is of the composite type with concrete caisson on a rubble mound. Two caissons were severly damaged due to the instability of a rubble mound.

Nondestructive Evaluation of Pavement

Nondestructive methods for evaluating the load carrying capacity of airport concrete pavements have been developed by using Falling Weight Deflectometer(FWD).

Seismic Damage to Gravity Quaywall

The 1983 Nipponkai-Chubu earthquake(Magnitude : 7.7)caused serious damage to port facilities in northern part of Japan. This photo shows the damage to gravity quaywall. The concrete cellular block walls were collapsed and completely submerged.

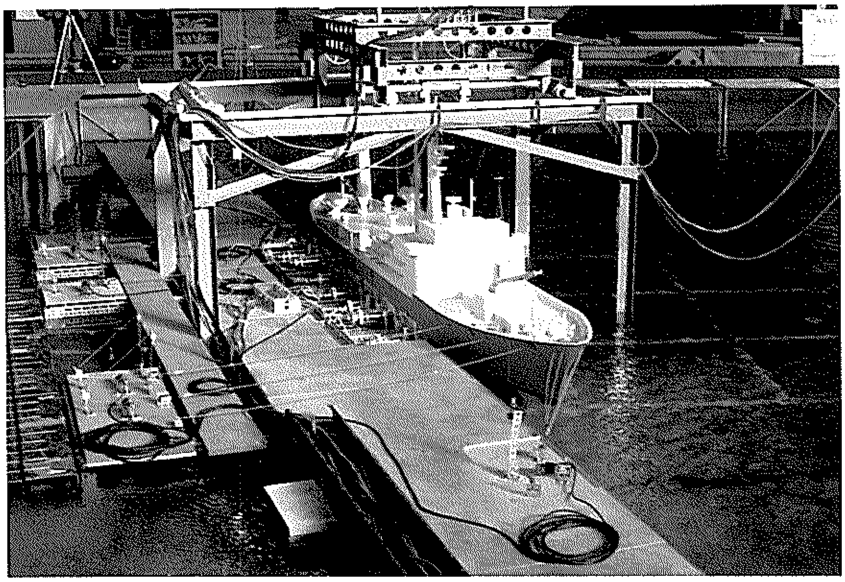

Model Experiment of Mooring Ship

Model ship is moored at a quay wall with fenders and mooring ropes subjected to gusty wind and/or irregular waves.

Vessel Congestion in Japan

As Japan is surrounded by the sea, there are many crowded water areas with various sizes and types of vessels. Arround there, many construction works were planned such as ports and harbours, off-shore airports, huge bridges and so on, so that many marine traffic observations and marine traffic simulations have been carried out.

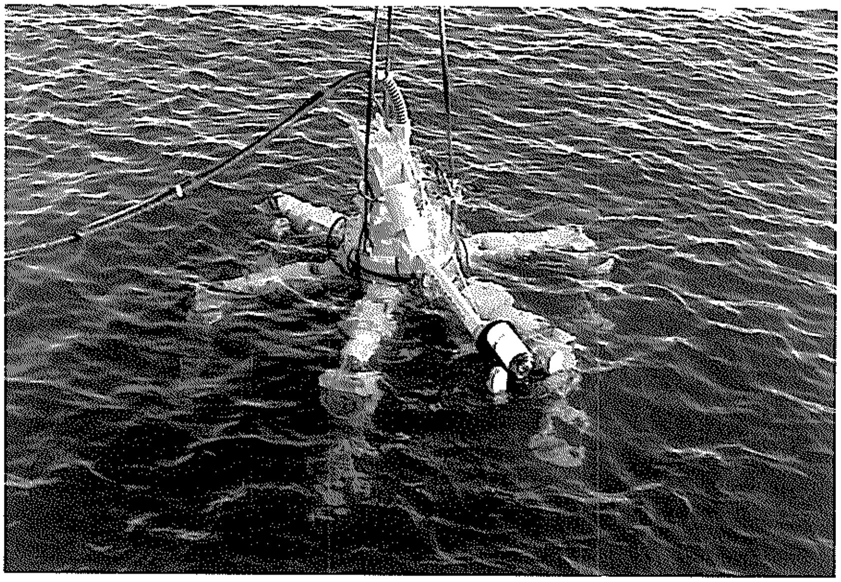

Underwater Inspection Robot

This is the six-legged articulated underwater inspection robot named "AQUAROBOT". The robot controlled by a computer can walk on uneven sea bed without making water muddy.

Foreword

The Port and Harbour Research Institute is a national laboratory under the Ministry of Transport, Japan. It is responsible for solving various engineering problems related to port and harbour projects so that governmental agencies in charge of port development can execute the projects smoothly and rationally. Its research activities also cover the studies on civil engineering facilities of air ports.

Last April we have celebrated the 25th anniversary of our institute because the present organization was established in 1962, though systematic research works on ports and harbours under the Ministry of Transport began in 1946. As an event for the celebration, we decided to publish a special edition of the Report of the Port and Harbour Research Institute, which contains full English papers only. These papers are so selected to introduce the versatility of our activities and engineering practices in Japan to overseas engineers and scientists. It is also intended to remedy to a certain extent the information gap between overseas colleagues and us.

The reader will find that our research fields cover physical oceanography, coastal and ocean engineering, geotechnical engineering, earthquake engineering, materials engineering, dredging technology and mechanical engineering, planning and systems analysis, and structural analysis. Such an expansion of the scope of research fields has been inevitable, because we are trying to cover every aspect of technical problems of ports and harbours as an integrated body.

The present volume contains eleven papers representing six research divisions of the institute. The materials introduced in these papers are not necessarily original in strict sense, as some parts have been published in Japanese in the Reports or the Technical Notes of the Port and Harbour Research Institute. Nevertheless they are all original papers in English and are given the full format accordingly. We expect that they will be referred to as usual where they deserve so.

It is my sincere wish that this special edition of the Report of the Port and Harbour Research Institute will bring overseas engineers and scientists more acquainted with our research activities and enhance the mutual cooperation for technology development related to ports and harbours.

December 1987
Yoshimi Goda
Director General

港湾技術研究所報告 (REPORT OF P. H. R. I.)

第26巻 第5号 (Vol. 26, No. 5) 1987年12月 (Dce. 1987)

目 次 (CONTENTS)

REPORT OF THE PORT AND
HARBOUR RESEARCH INSTITUTE
Vol. 26, No. 5 (Dec. 1987)

5. Modeling for the Prediction of the Effects of Sea Bed Sediment Treatment on the Improvements of Ecological Conditions and Seawater Quality

Takeshi HORIE*

Synopsis

This paper deals with the development of a numerical model for predicting the effect of purification countermeasures in polluted seas on the improvement of seawater quality and sea bed sediment, and on the recovery of marine animals. The present model includes biological processes such as zooplankton, benthos and periphyton activities, as well as the processes of seawater circulation, dispersion, settling, the production of organic matter and its decomposition, release rate, etc., which have already been contained to the existing model. The present model can predict the the effect of sea bed sediment treatment on such biological aspects as the increase of biological mass and biological activities.

The present study indicates that the seasonal variation of seawater quality, seabed sediment in polluted seas, and of plankton, periphyton, and oysters, etc. can be estimated by the nutrient cycle model of a phosphorus tracer. The calibration test for this model is made for the case of the bay of Kure in Horishima Prefecture. The spatial treatment of the calibration test is a uni-segment and eleven layers. According to the calibration results, the seasonal variation of phosphate phosphorus (PO_4-P) and dissolved oxygen (DO) agrees well with the observed data, and the standing crop of phytoplankton and benthos is the agreeable value, but the abrupt increase of phytoplankton observed around June is not well reproduced. The biomass of the calculated zooplankton exceeds the observed values during the term between December to February.

This model is found to be a practical tool to estimate, from the viewpoint of biological aspect, the effect of the sediment treatment on the release-cut-off, and on the biological activities, which result from changes in the grain size of the sediment, and the recovery of benthos and bottom fish.

* Chief of Purification Hydraulics Laboratory, Marine Hydrodynamics Division

港湾技術研究所報告
第26巻 第5号 (1987.12)

5. 海域底泥の改良による生態系と水質の改善効果予測の数値解法

堀 江 毅*

要 旨

汚染海域の浄化対策による水質・底質浄化効果，および，生物の回復効果を予測するため，従来のモデル—すなわち，海水の流れ，拡散，沈降に伴う物質輸送，有機物の生産と分解，溶出などの過程を取り込んだモデル—に対して，さらに，動物プランクトン，底生生物，付着生物カキ等の生物過程を加え，底質処理のほか，海域の浄化対策による浄化効果を生物の活性，現存量の増加等の生物学的な面からの効果と合わせ評価することのできるモデルの開発を行った。

本研究において，汚染海域の水質・底質，プランクトン，底生生物，カキなどの現存量を，リンを指標とする物質循環モデルで再現できることを示した。このモデルを呉湾を対象とした1ボックス，11層モデルに適用した結果，リン酸態リン，溶存酸素については季節変化を含め再現性は良好であった。植物プランクトンとベントスとは，年平均的な現存量はほぼ再現された。しかし，6月付近にみられる植物プランクトンのピーク値の再現にはなお検討の余地が残された。動物プランクトンについては，12～2月において計算値が上回った。

本モデルは，底質浄化による溶出抑制効果，底質粒度変化に伴う生物活性効果などをとりいれることにより，ベントスや底魚の現存量の増加などといった生物学的な観点から評価する手段として利用できる可能性が示された。

* 海洋水理部 海水浄化研究室長

Contents

1. Introduction

The Ports and Harbours Construction Bureau of the Ministry of Transport, Japan has been carrying out an overall investigation on countermeasures to minimize the seawater pollution in inland seas or inner bays. Seawater pollution due to organic compounds is mainly caused by such processes as effluent, internal production and release from the seabed sediment. These processes are quite influential to the seawater quality, and interact complicatedly with each other. The release from the sediment is determined by the sediment property, temperature, overlaying dissolved oxygen, etc. The cut-off of the release by the dredging of the seabed sediment or by the capping with clean materials, as well as the control of effluent load due to urban, agricultural, and industrial sewages, seems to be an effective method for the improvement of eutrophic seawater quality. However, the volume of the treated sediment must be minimized for reasons of economy.

The feasibility studies on seawater improvement projects are carried out for selected bays where the seawater is highly polluted by organic substances. In accordance with the above purposes, such field surveys as seawater quality, sediment quality, release rate, growth rate, and biological activities were conducted for those bays. The release-cut-off effect due to the dredging of the sediment or the capping with the clean materials was then observed in the field.

At the same time, numerical analysis is also made by using a set of mathematical models. A water quality prediction model is built on the basis of the phosphorus cycle between seawater, phytoplankton and sediment. The phosphorus cycle in the model is formulated by the processes of the inner production, decomposition, settling, advection and dispersion. The effect on water quality improvement, release-cut-off, and sediment improvement is predicted by the above model.

According to the simulation results, the effect of sediment dredging or capping with clean materials can be expected for some period, but the release rate gradually increases with the elapse of time owing to the newly deposited materials. The apparent effect of water quality improvement is unexpectedly small because of dilution due to advection, and dispersion by seawater circulation. However, the ecological conditions seem to be significantly improved in the field, in consideration of the fact that the number of benthos' species and its population increases for the treated sediment, even though the improvement effect for the water quality was less than expected. Furthermore, the improvement effect should be discussed not only for organic substances, but also for dissolved oxygen. To cope with this problem, a more elaborated model is required.

The present paper describes the review of previous investigations on seawater quality and seabed sediment in the first paragraph, particularly for numerical approaches. The role of ecological processes in seawater and sediment are then described in connection with plankton, benthos and periphyton. The numerical modeling of such ecological processes is explained by indicating assumptions for the model formulation, basic equations, and the simulation procedures. The model developed here is calibrated by application to Kure Bay. Finally, the reliability and the improvement items to the model are investigated.

2. Review of the Previous Investigations on Seawater Quality and Seabed Sediment

2.1 The role of the numerical model

As the tool to predict the improvement effect, laboratory tests, field surveys and numerical models are available. Laboratory tests are quite important to the analysis of phenomena which control the processes of the organic pollution in bays. For instance, the phytoplankton growth rate is formulated by laboratory tests with different conditions of illumination, temperature and nutrient concentration. The decomposition rate of organic matter is also formulated by data obtained in laboratory tests. In the same manner, the oxygen uptake rate of the sediment and the nutrient adsorption/desorption rate are formulated by data obtained in laboratory tests where the temperature and dissolved oxygen are controlled. However, in general, the similarity of phenomena between in confined-small-scale capsule and in the natural field is not always satisfactory. Especially, experiments of the phenomena concerned with biological activities encounter many problems because the experimental conditions between the capsule and the field differ greatly.

On the other hand, field experiments can be performed at the actual scale under natural conditions, such as for field experiments on the settling rate, the suspension rate, growth rate, etc. Though data obtained by the field experiment are of the prototype, a lot of data with different conditions are necessary to build a certain formula. In other words, field experiments are carried out at so big scale that the experimental conditions cannot be easily controlled. Therefore, the number of experimental runs and the scale of the experiment are restricted for reasons of time and cost. For the effective determination of the phenomena, the roles of laboratory tests and field experiments should complement with each other. The phenomena which concern chemical reactions or biological activities occur at the same rate and at real time, regardless of the model scale, and cannot be arbitrarily controlled.

Numerical models play a great role in compensating for the demerits of laboratory tests and field experiments. Numerical models, however, rely greatly on these results because the model is formulated by data obtained through laboratory tests and field experiments. In other words, the reliability of numerical models depends solely on the certainty of the data obtained by laboratory tests and field experiments.

2.2 Existing nutrient cycle model

Phenomena occurring in the field are not always treated in the model, but are selectively treated for the reason of simplification to correspond to the purpose of prediction. Prediction models which treat the composition and the decomposition of organic substances is classified into two categories: ecological dynamics model and nutrient cycle model. The ecological dynamics models treat species and the population of individual organisms. Namely, the model treats the mutual relations between inorganic nutrients, phytoplankton, zooplankton, detritus, etc., and estimates their stocks in consideration of the nutrient budget. Thus, as the number of parameters treated in the model is increased, the number of variables which determine the nutrient cycle rates is also increased. Among those variables, parameters related to biological activity are determined only with the greatest effort. Therefore, even if a more elaborated model is built while the above mentioned processes are still uncertain, the result produced by the model is then not necessarily reliable.

On the other hand, the nutrient cycle model handles the mutual nutrient budget between inorganics and organics. In this way, the nutrient budget between inorganics and organics is formulated to such a simple relation as composition and decomposition. It would be ideal to formulate each process to the ecological dynamics model and to analyze the mutual relations between the seawater, the sediment and animals. However, the ecological dynamics model has no evidence that it estimates such complicated relations with high reliability. From this reason, the previous nutrient cycle model is developed for the prediction of the effect of the sediment treatment on seawater quality.

2.3 Phosphorus as the tracer of the model

Phosphorus and nitrogen compounds are most important nutrients which control seawater pollution by organics. The content of phosphorus and nitrogen in organics is generally kept in a certain ratio, but this ratio differs between species of organisms or the stage of their growth. Therefore, the nutrient budget is determined by both phosphorus and nitrogen. The structure of the prediction model, however, becomes more complicated if both nitrogen and phosphorus behaviors are formulated. Thus, the nutrient cycle treated by only phosphorus is preferentially applied to the previous analysis for the reason that the phosphorus would be a limiting factor to the nutrient cycle in eutrophic bays. The following assumptions are built into the formulation of the nutrient cycle model in seawater: i) the system controlling process of the nutrient cycle is treated as the growth and decomposition between phosphate phosphorus (PO_4–P) and organic phosphorus (O–P), and dissolved oxygen (DO) generates to correspond to the basic process, ii) COD, DO, PO_4–P and DO are used as the indices of the seawater quality, iii) the growth of the phytoplankton occurs only in the photic layer, iv) COD, DO and phosphorus concentrations vary through the processes of the growth, the decomposition, the release, the settlement, etc., and v) the above indices are varied with advection and dispersion due to seawater circulation.

To the nutrient cycle in the sediment, the following assumptions are incorporated: vi) both the O–P supplied from seawater and the O–P in the sediment are decomposed into PO_4–P, vii) the decomposed PO_4–P is allocated, with a certain ratio, to the interstitial water and sediment particles, viii) the interstitial PO_4–P and O–P are transported in the sediment by adsorption/desorption, dispersion, bioturbance, etc., ix) PO_4–P release is occurred by dispersion.

2.4 Basic equations of the nutrient cycle model

(1) Seawater quality model

Under the assumptions stated above, the O–P, PO_4–P, COD, and DO in each layer are related as shown in Fig. 1 and their time variations are expressed in the three-layer model as follows:

Time variation of each concentration in each layer

= horizontal advection (T_{HA})
+ vertical advection (T_{VA})
+ horizontal dispersion (T_{HD})
+ vertical dispersion (T_{VD})

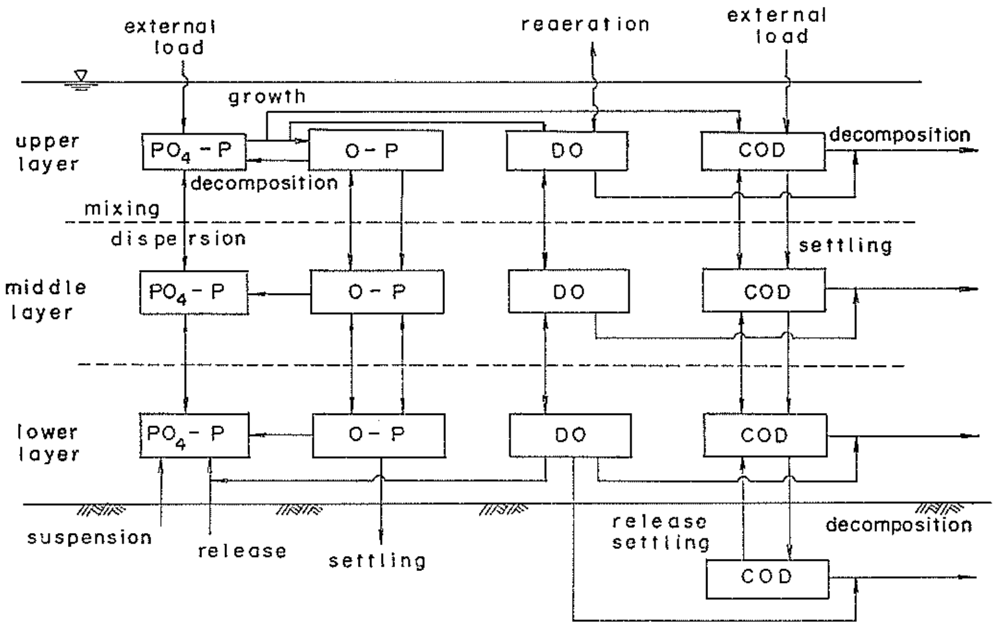

Fig. 1 Nutrient Cycle Model to the Seawater System

+ growth (T_G)
+ decomposition (T_B)
+ settling (T_S)
+ release (T_R)
+ external load (T_L)
+ uptake by sediment (T_C)
+ exchange with the atmosphere (T_E) (1)

The left hand side of Eq. (1) is expressed as

$$\frac{d(M_iD_i)}{dt} \tag{2}$$

where M_i indicates the concentration of the index i (O–P, PO_4–P, COD, DO), D_i the thickness of layer i, and t time. The first term of the right hand side is the horizontal advection and is expressed as

$$-\frac{\partial}{\partial x}(u_iM_iD_i)-\frac{\partial}{\partial y}(v_iM_iD_i) \tag{3}$$

where u_i and v_i indicate the seawater circulation components of each layer i. The second term of the right hand side is expressed as

$$\frac{\partial}{\partial x}\left(K_iD_i\frac{\partial M_i}{\partial x}\right)+\frac{\partial}{\partial y}\left(K_iD_i\frac{\partial M_i}{\partial y}\right) \tag{4}$$

where K_i denotes the horizontal dispersion coefficient in layer i. The rest terms of Eq. (1) are listed in Table 1.

Table 1 Terms of the Nutrient Cycle Model to Seawater System

		upper layer	middle layer	lower layer
O-P	T_{VA}	$w_{3/2} \cdot OP^*$	$-w_{3/2} \cdot OP^* + w_{5/2} \cdot OP^{**}$	$-w_{5/2} \cdot OP^{**}$
	T_{VD}	$-K_z(OP_1 - OP_2)$	$K_z(OP_1 - OP_2) - K_z(OP_2 - OP_3)$	$K_z(OP_2 - OP_3)$
	T_G	$G \cdot OP_1 \cdot D_1$	$G \cdot OP_2 \cdot D_2$	0
	T_B	$-B_1{}^P \cdot OP_1 \cdot D_1$	$-B_2{}^P \cdot OP_2 \cdot D_2$	$-B_3{}^P \cdot OP_3 \cdot D_3$
	T_S	$-S_1{}^P \cdot OP_1$	$S_1{}^P \cdot OP_1 - S_2{}^P \cdot OP_2$	$S_2{}^P \cdot OP_2 - S_3{}^P \cdot OP_3$
	T_L	L_{OP}	0	0
	T_R, T_C, T_E	0	0	0
PO_4-P	T_{VA}	$w_{3/2} \cdot IP^*$	$-w_{3/2} \cdot IP^* + w_{5/2} \cdot IP^{**}$	$-w_{5/2} \cdot IP^{**}$
	T_{VD}	$-K_z(IP_1 - IP_2)$	$K_z(IP_1 - IP_2) - K_z(IP_2 - IP_3)$	$K_z(IP_2 - IP_3)$
	T_G	$-G \cdot OP_1 \cdot D_1$	$-G \cdot OP_2 \cdot D_2$	0
	T_B	$B_1{}^P \cdot OP_1 \cdot D_1$	$B_2{}^P \cdot OP_2 \cdot D_2$	$B_3{}^P \cdot OP_3 \cdot D_3$
	T_R	0	0	R_{IP}
	T_L	L_{IP}	0	0
	T_S, T_C, T_E	0	0	0
COD	T_{VA}	$w_{3/2} \cdot COD^*$	$-w_{3/2} \cdot COD^* + w_{5/2} \cdot COD^{**}$	$-w_{5/2} \cdot COD^{**}$
	T_{VD}	$-K_z(OP_1 - OP_2)$	$K_z(OP_1 - OP_2) - K_z(OP_2 - OP_3)$	$K_z(OP_2 - OP_3)$
	T_G	$\beta \cdot G \cdot OP_1 \cdot D_1$	$\beta \cdot G \cdot OP_2 \cdot D_2$	0
	T_B	$-B_1{}^C \cdot COD_1 \cdot D_1$	$-B_2{}^C \cdot COD_2 \cdot D_2$	$-B_3{}^C \cdot COD_3 \cdot D_3$
	T_S	$-S_1{}^C \cdot DOD_1$	$S_1{}^C \cdot COD_1 - S_2{}^C \cdot COD_2$	$S_2{}^C \cdot COD_2 - S_3{}^C \cdot COD_3$
	T_R	0	0	R_{COD}
	T_L	L_{COD}	0	0
	T_C, T_E	0	0	0
DO	T_{VA}	$w_{3/2} \cdot DO^*$	$-w_{3/2} \cdot DO^* + w_{5/2} \cdot DO^{**}$	$-w_{5/2} \cdot DO^{**}$
	T_{VD}	$-K_z(DO_1 - DO_2)$	$K_z(DO_1 - DO_2) - K_z(DO_2 - DO_3)$	$K_z(DO_2 - DO_3)$
	T_G	$\gamma \cdot G \cdot OP_1 \cdot D_1$	$\gamma \cdot G \cdot OP_2 \cdot D_2$	0
	T_B	$-B_1{}^O \cdot COD_1 \cdot D_1$	$-B_2{}^O \cdot COD_2 \cdot D_2$	$-B_3{}^O \cdot COD_3 \cdot D$
	T_C	0	0	DB
	T_E	$A(HOWA - DO_1)$	0	0
	T_S, T_R, T_L	0	0	0

Parameters appeared in Table 1 are explained as follows:

$w_{3/2}$, $w_{5/2}$: vertical velocity components of seawater circulation in the interface between the upper layer and the middle layer, and the middle layer and the lower layer, respectively

K_z : vertical dispersion coefficient

G : growth rate of phytoplankton

$B_i{}^C$: COD decomposition rate in layer i

$B_i{}^O$: oxygen uptake rate by the decomposition in layer i

$S_i{}^P$: O–P settling rate in layer i

$S_i{}^C$: COD settling rate in layer i

R_{IP} : PO_4–P release rate

L_{OP} : O–P external load

L_{IP}	:	I–P external load
L_{COD}	:	COD external load
A	:	reaeration constant
$HOWA$	:	saturated oxygen concentration
DB	:	oxygen uptake rate by seabed sediment
β	:	COD conversion factor
γ	:	DO conversion factor

The parameters which contain asterisks indicate that

$$OP^{*}=OP_2,\ IP^{*}=IP_2,\ COD^{*}=COD_2,\ DO^{*}=DO_2 \text{ for } w_{3/2}\geqq 0,$$
$$OP^{*}=OP_1,\ IP^{*}=IP_1,\ COD^{*}=COD_1,\ DO^{*}=DO_1 \text{ for } w_{3/2}<0,$$
$$OP^{**}=OP_3,\ IP^{**}=IP_3,\ COD^{**}=COD_3,\ DO^{**}=DO_3 \text{ for } w_{5/2}\geqq 0,$$
$$OP^{**}=OP_2,\ IP^{**}=IP_2,\ COD^{**}=COD_2\ DO^{**}=DO_2 \text{ for } w_{5/2}<0,$$

respectively.

Eq. (1) is transformed into a finite difference equation. Thus, the O–P, PO_4–P, COD, and DO concentrations in each layer and each time stage is calculated by the set of difference equations.

(2) Seabed sediment model

Based on the assumptions stated at the previous paragraph, the seabed sediment model is formulated to the O–P, inorganic phosphorus (I–P) in the sediment, and interstitial PO_4–P are related as shown in Fig. 2, and their concentrations at each time stage in each layer are expressed as follows:

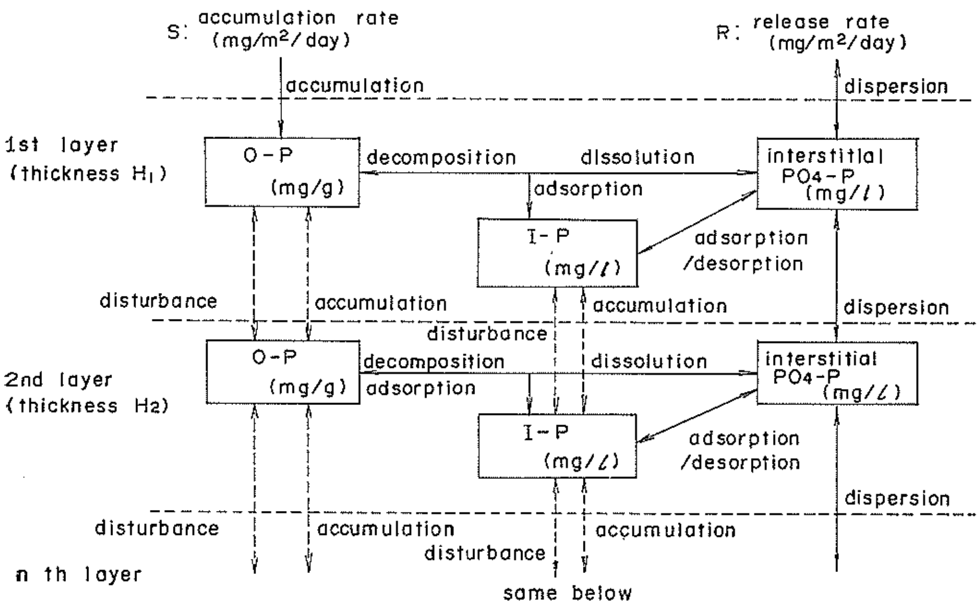

Fig. 2 Nutrient Cycle Model to the Sediment System

$$OP_n^{t+1}-OP_n^t=\{\underbrace{-r_n^t}_{\text{decomposition}}+\underbrace{DS\times(OP_{n-1}^t-OP_n^t)}_{\text{accumulation}}$$
$$+\underbrace{DSL\times(OP_{n-1}^t-2\times OP_n^t+OP_{n+1}^t)}_{\text{agitation}}\}\times\Delta t \quad (5)$$

for O–P in the n-th layer.

$$IP_n^{t+1}-IP_n^t=\Bigg\{\underbrace{\frac{1/\phi_n\alpha_n}{1+(1/\phi_n\alpha_n)}\times r_n^t}_{\text{allocation}}+\underbrace{q_n^n}_{\text{adsorption/ desportion}}+\underbrace{DS\times(IP_{n-1}^t-IP_n^t)}_{\text{accumulation}}$$
$$\underbrace{+DSL\times(IP_{n-1}^t-2\times IP_n^t+IP_{n+1}^t)}_{\text{agiation}}\Bigg\}\times\Delta t \quad (6)$$

for I–P in the n-th layer.

$$C_{*1}^{t+1}-C_{*1}^t=\Bigg[\underbrace{\frac{1}{1+(1/\phi_1\alpha_1)}\times\frac{1}{\phi_1}\times r_1^t}_{\text{allocation}}-\underbrace{\frac{1}{\phi_1}\times q_1^t}_{\text{adsorption/ description}}+\Bigg\{\underbrace{\phi_1'\times D\times\frac{C_w^t-C_{*1}^t}{H_1/2}}_{\text{dispersion}}$$
$$\underbrace{+\phi_1'\times D\times\frac{C_{*2}^t-C_{*1}^t}{(H_1+H_2)/2}}_{\text{dispersion}}\Bigg\}\times\frac{1}{H_1}\Bigg]\times\Delta t \quad (7)$$

for c_{*1} in the 1st layer.

$$C_{*n}^{t+1}-C_{*n}^t=\Bigg[\frac{1}{1+(1/\phi_n\alpha_n)}\times\frac{1}{\phi_n}\times r_n^t-\frac{1}{\phi_n}\times q_n^t$$
$$+\Bigg\{\phi_n'\times D\times\frac{C_{*n-1}^t-C_{*n}^t}{(H_n+H_{n-1})/2}+\phi'_{n+1}\times D\times\frac{C_{*n+1}^t-C_{*n}^t}{(H_{n+1}+H_{n-1})/2}\Bigg\}$$
$$\times\frac{1}{H_n}\Bigg]\times\Delta t \quad (8)$$

for C_{*n} in the n-th layer.

$$C_w^{t+1}=\left(C_w^t+\frac{1}{1000}\times R^t\times\Delta t\right)\times DL \quad (9)$$

for C_w in the overlaying layer.
where OP: O–P (mg/g), IP: I–P (mg/g), C_*: interstitial PO_4–P (mg/l), C_w: overlaying PO_4–P (mg/l), r: O–P decomposition rate (mg/g/day), DS: O–P settling rate (1/day), DSL: bioturbance coefficient (m^2/day), D: PO_4–P dispersion coefficient (m^2/day), ϕ: interstitial water ratio in dry sediment, ϕ': void ratio, α: allocation coefficient (g/l), H: layer thickness (m). The superscription and subscription of each variable denote the time stage and the layer, respectively. The fourth term in the right hand side of Eq. (9) implies the release rate expressed as:

$$R=-\phi'\times D\times\frac{C_w-C_{*1}}{H_{1/2}}\times 1000\ (\text{mg/m}^2/\text{day}) \quad (10)$$

2.5 Prediction of the improvement effect of the sediment treatment on seawater quality and nutrient release rate

(1) Prediction of the effect of sediment treatment on seawater quality

The model stated above was calibrated to several bays and found to be practical[1),2)]. By using this model, the following simulation is carried out with respect to predicting the effect of sediment treatment on the seawater quality in Kure Bay. The computation area covers about 20 km in the east-westward and 30 km in the north-southward as shown in Fig. 3, and is horizontally divided into 500 m× 500 m grids. The number of the vertical layers is basically three: 5 m in thickness in the upper layer and 5 m in thickness in the middle layer. However, in the zone where the water depth does not exceed 5 m, the middle layer and the lower layer

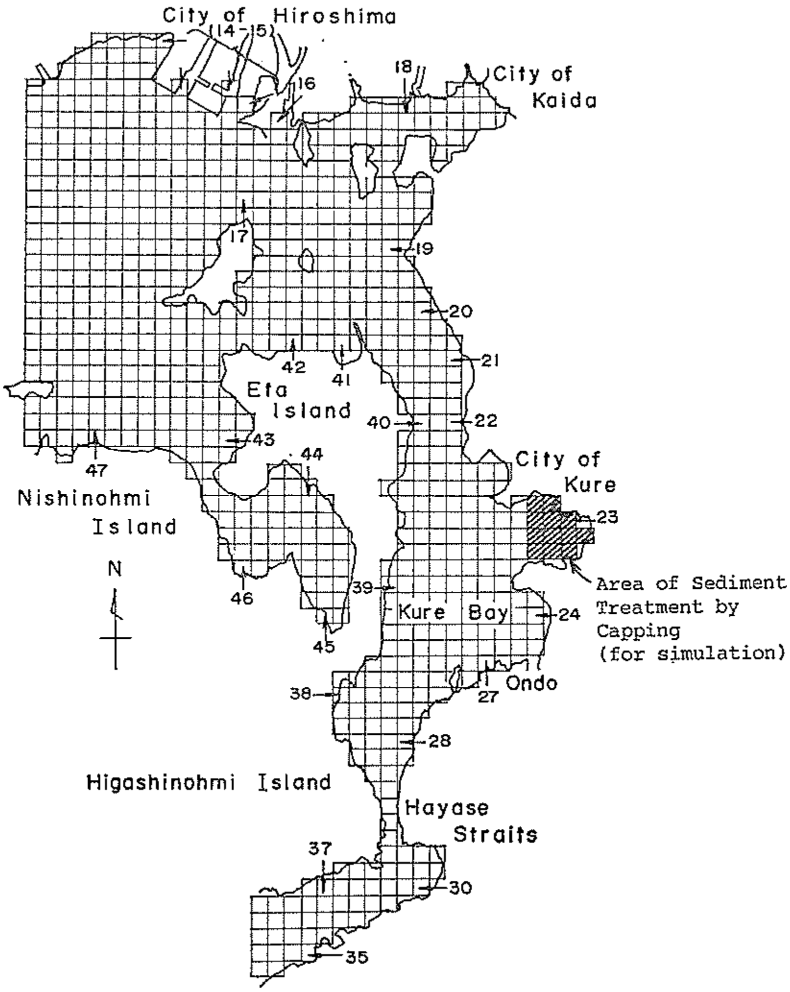

Fig. 3 Computational Area (arrow and number show the points of external load injection)

Table 2 Computational Conditions to the Present State of Kure Bay

Item		Value		
layer thickness		upper layer: 5 m, middle layer: 5 m		
growth rate (1/day)		$0.489 \times \frac{IP}{0.027+IP}$ to the upper layer		
O-P decomposition rate (1/day)		upper 0.04	middle 0.04	lower 0.04
COD decomposition rate (1/day)		0.014	0.014	0.018
DO uptake rate by decomposition ($mg/m^2/day$)		0.078	0.078	0.067
O-P settling rate (m/day)		0.284	0.264	0.792
COD settling rate (m/day)		0.325	0.325	0.650
DO uptake rate by sediment ($mg/m^2/day$)		from 390 to 1000		
COD release rate ($mg/m^2/day$)		from 44 to 49		
PO_4-P release rate ($mg/m^2/day$)		from 7 to 33		
boundary treatment		dilution coefficient 0.999 however, DO fixed 8 mg/l in the upper and the middle layers, but 6.0 mg/l in the lower layer		
effluent load		from 27 points about 67 t/day of COD, and 2.8 t/day of T-P		
COD conversion coefficient		71.0		
DO conversion coefficient		143		
reaeration (1/day)		0.1		
dispersion coefficient (cm^2/s)		10^4		
initial value (mg/l)		upper layer	middle layer	lower layer
	O-P	0.04	0.04	0.04
	PO_4-P	0.0	0.0	0.0
	COD	1.4	1.4	1.4
	DO	8.0	8.0	6.0
time increment		720 second		
computation time		for 120 tidal repetetion		

disappear, and in the zone where the water depth is more than 5 m but less than 10 m, the lower layer disappears. The seawater circulation which displays the great influence to the seawater quality in the bay is determined by the three layer model. The values at open boundaries are obtained by the precedent computation in the greater grid of the wider area. The target of the seawater quality is obtained by processing field data observed by the local government for July, August and September in the past five years.

The total external loads in the computational area are, COD 7.3 t/d, PO_4–P 0.4 t/d, O–P 0.1 t/d, respectively. The release rates of PO_4–P and COD from the sediment are determined by the function of temperature, DO and the sediment properties. Consequently, the PO_4–P release rate distributes from 7 to 33 mg/m^2/d, and COD from 44 to 49 mg/m^2/d. The parameters applied to the model are mostly obtained by laboratory tests and field surveys, and are shown in Table 2. In general, the simulation result of the water quality distribution agrees well with the target.

Sediments containing COD greater than 30 mg/g–SS in the surface layer are distributed almost all over the bay. The COD content in the sediment here is comparable to that of inner Tokyo Bay or Osaka Bay.

As one of the sediment treatments in Kure Bay, the capping method is investigated for the area about 300 ha near Kure City as shown by hatching in Fig. 3. The release rate in the treated area is assumed to be zero in this simulation.

The COD variation in the upper layer is shown in Fig. 4 on the basis of the corresponding COD in the present condition. The greater negative values in Fig. 4 imply the greater improvement of seawater quality due to sediment treatment. The balance of the improved seawater to the present seawater is about 0.2 to 0.3 mg/l in the sediment treated area, and decreases away from the treated site. The COD in the middle layer and the lower layer display the same features as the upper layer. However, the improvement of PO_4–P and O–P is very small and does not

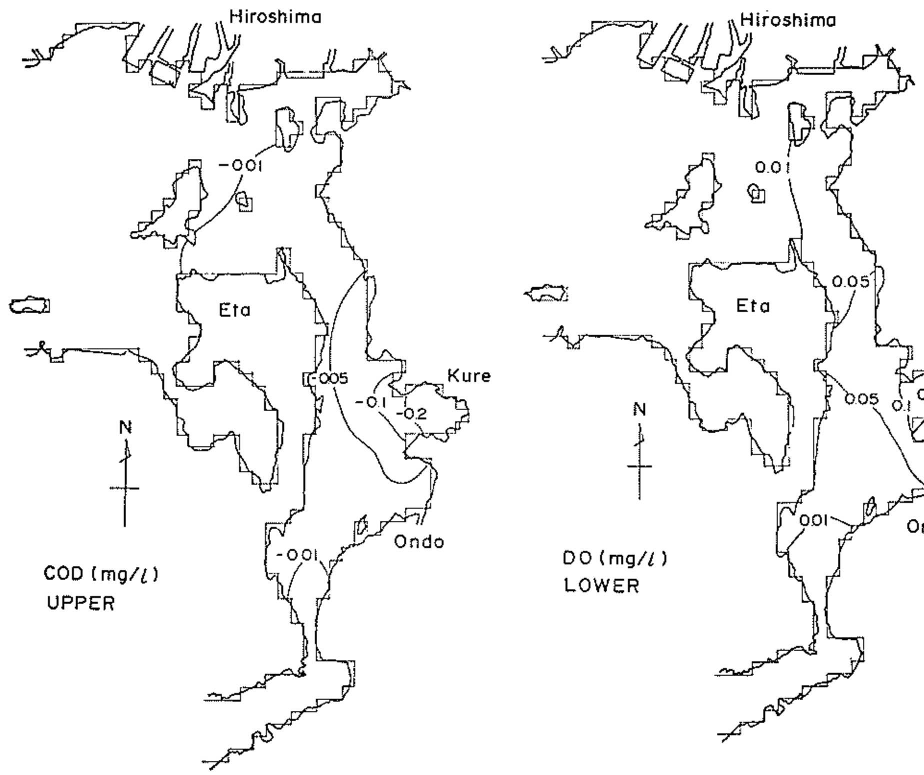

Fig. 4 COD and DO Improvement (COD: upper, DO: lower)

appear to the magnitude of 10^{-3}mg/l. On the other hand, DO increases by about 1 mg/l around the treatment site in the whole layers; and is especially greater in the lower layer. This means that the DO uptake by the sediment is decreased by capping with clean materials.

Generally speaking, the improvement effect of such sediment treatment on the seawater quality is unexpectedly small.

(2) Prediction of the effect of seabed sediment on the release rate

The seabed sediment model stated at the previous section is also applied to the data for Kure Bay. According to the observation data for a certain point in the bay, the PO_4–P release rate is about 10 mg/m²/d in the period from June to October and about 5 mg/m²/d or less in the winter, and about 2 g/m²/year. The vertical distribution of T–P in the sediment is higher in the layer within 30 cm in depth from the bed surface and almost constant in the deeper layer. The vertical distributions of O–P in the sediment and interstitial PO_4–P also display a similar profile. However, the I–P content in the sediment is nearly constant throughout the layer. By using the above data and constants listed in Table 3, the vertical distribution of nutrients in the sediment is simulated by the increment time of 0.1 day. Figure 5 shows the simulation results of the calculated T–P, O–P, I–P, interstitial PO_4–P,

Table 3 Computational Conditions to the Capping

Item	Value or function	
Settling rate	5.4 g-SS/m²/day	correspond to the accumlation rate of 0.67 cm/year for the sediment of water content 0.756 and unit weight 1.21 g/cm³
Phosphorus in settling substance	1.7 mg-P/g-SS { O-P 72% (1.22 mg-P/ig-SS) { I-P 28% (0.48 mg-P/g-SS)	
thickness of the surface layer	0.7 cm	correspond to one year accumlation
decomposition rate of the fresh sediment	$r_F=0.023\times(\text{O-P/SS}-0.61)\times1.07^{T-25}$ (mg-P/g-SS/day)	T : water temperature (℃)
decomposition rate of the bottom sediment (mg-P/g-SS/day)	$r_s=0.0012\times(\text{O-P/SS}-0.31)\times1.07^{T-25}$ for 0.7～5 cm layer $r_s=0.00091\times(\text{O-P/SS}-0.31)\times1.07^{T-25}$ for 5～10 cm layer $r_s=0.00025\times(\text{O-P/SS}-0.31)\times1.07^{T-25}$ for the lower layer	T : water temperature (℃)
allocation factor	$22.3\times0.717^{DO}\times1.02^{T-20}$ (g/l)	DO : the overlaying DO concentration (mg/l) T : water temperature (℃)
dispersion coefficient	$9.9\times10^{-5}\times1.03^{T-25}$ (m²/day)	T : water temperature (℃) correspond to 1.1×10^{-5}cm²/s for $T=25$℃
bioturbation coefficent	3.4×10^{-6} (m²/day)	correspond to the fully mixing of 15 cm thickness for four years

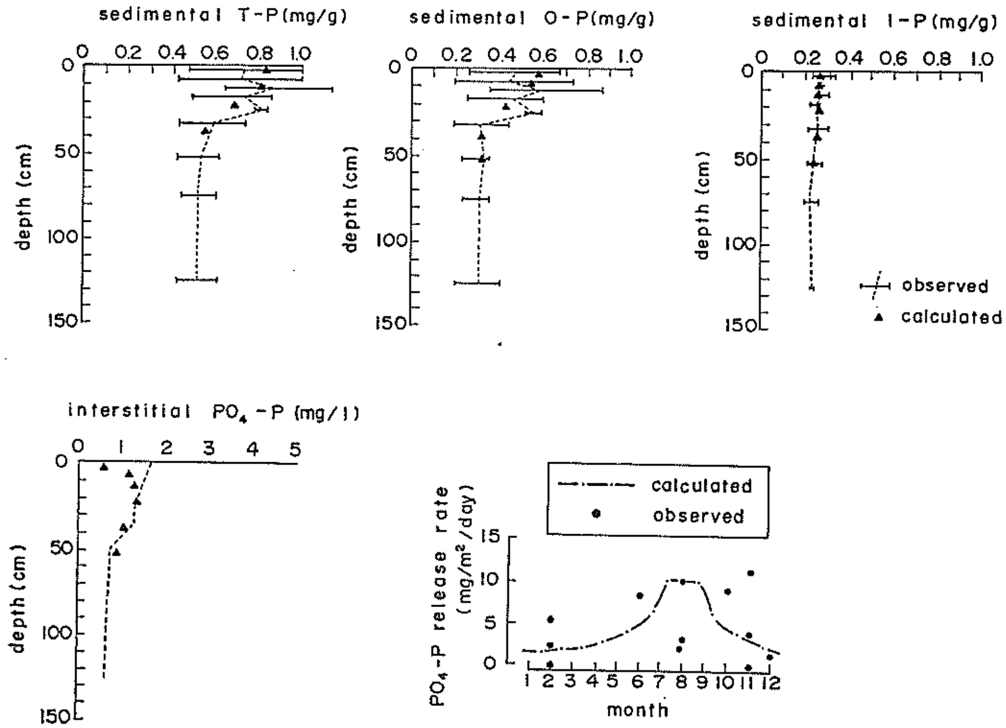

Fig. 5 Calibration of the Sediment Model

PO_4–P release rate and the corresponding observed values. The calculated values agree satisfactorily with the observed values.

This model is again applied to the prediction of the effect of capping with clean materials on PO_4–P release control. On the capping simulation, the following items are considered as the conditions which vary with the sediment treatment:

i) the capping is carried out by clean material overlaid on the existing seabed sediment, and the thickness of the material is 30 cm.

ii) the existing sediment is consolidated by the load of the material. The interstitial water in the sediment is reduced by this consolidation, but the interstitial PO_4–P is conservative.

iii) the substances deposited after capping is contained in the pore of the material until the pore is filled entirely with the substance, and is then deposited on the material.

The variation of the porosity (ϕ') and the water content (ϕ) due to the consolidation is modified in consideration of the difference of the unit weight between the material and the sediment. The grain size accumulation curve of the material and sediment are shown in Fig. 6.

The computation results concerning the release rate are shown in Fig. 7. According to these results, the PO_4–P release rate is controlled in the lower level for the first five to eighteen years owing to the capping effect, and gradually increased as the sediment pore is filled with the deposited substances. The release rate

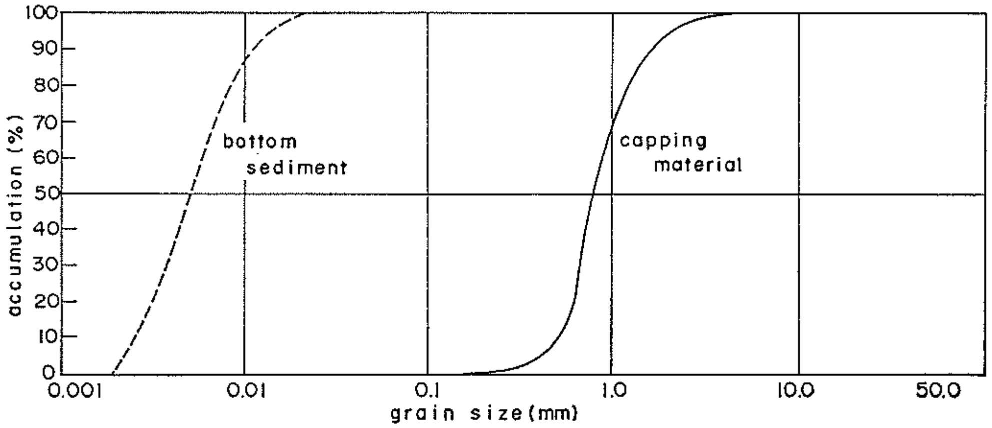

Fig. 6 Accumulation Curve of the Sea-bed Sediment and the Capping Material

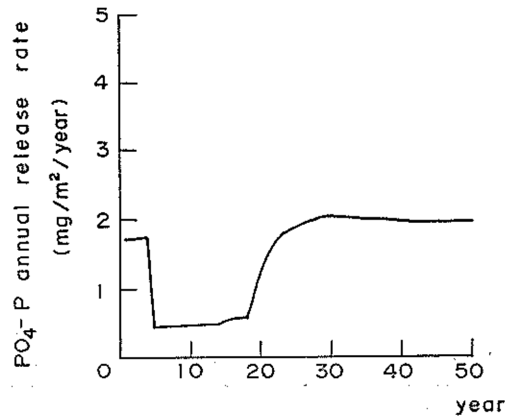

Fig. 7 Predicted Release Control Effect

keeps nearly constant values over 22 years.

For the present investigation, the release-cut-off due to capping is very effective for the first fifteen years. However, the effect is reduced if the settling rate from the seawater keeps constant with the present rate.

3. Numerical Modeling of Ecological Processes

3.1 Evaluation of the effect from ecological aspects

As stated in 2.5, the apparent effect of the sediment treatment on the seawater quality is very small because of dilution and dispersion due to seawater circulation. This means that a huge scale of the treatment, such as the capping all over the bay, is required for attaining a clear effect on the seawater quality. This also means that a huge cost is required. However, such a huge scale treatment is almost

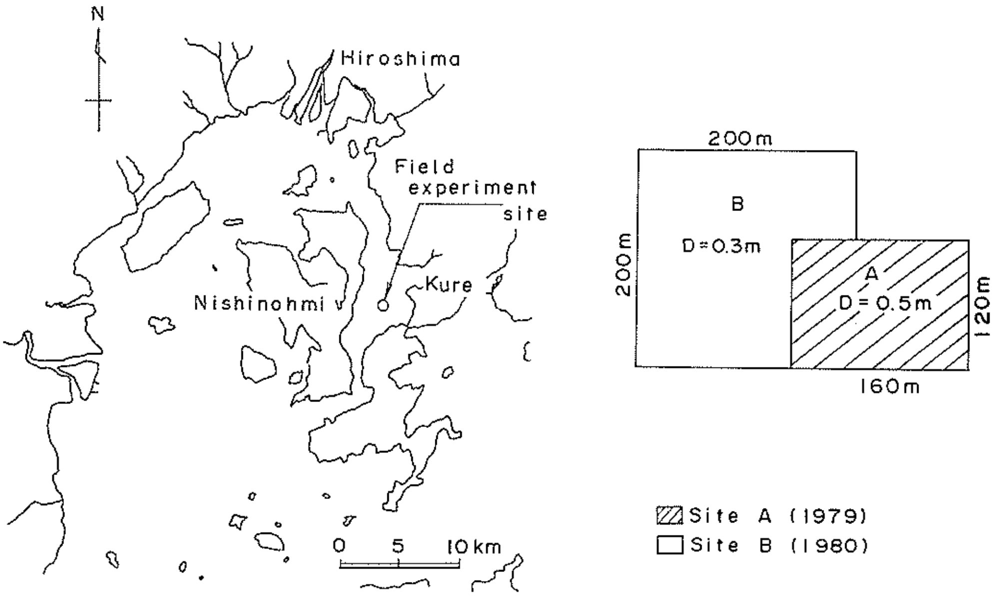

site	site A	site B
experimental period	Oct-Nov 1979	July-Aug 1980
experimental scale	capping 1.92ha(120m x 160m) 0.5m in thickness	capping 4.48ha (200m x 200m + 80m x 60m) 0.3m in thickness
material	sea-bed sand	sea-bed sand

Fig. 8 Field Experiment Sites in Kure Bay

impossible to be carried out in a short period from the viewpoint of technological and economical reasons. Thus, another evaluation methodology should be found for the recognition of the necessity of reasonable treatment, and an ecological approach is often helpful.

The Third District Port Construction Bureau, Ministry of Transport, is carrying out a field investigation on the recovery of sea animals around the seabed treatment site in Kure Bay (see Fig. 8). The treatment was carried out twice; in October to November in 1979, and in July to August in 1980. The treatment is by capping, and the area was 1.92 ha and 0.5 m in thickness for the first one (Site A), and 4.48 ha in area and 0.3 m in thickness (Site B), respectively. The benthos was observed inside and outside the treated sites for about four years after the treatment. Figure 9 shows the observation results for the benthos. According to Fig. 9, the number of benthos is less in summer both inside and outside the treatment sites.

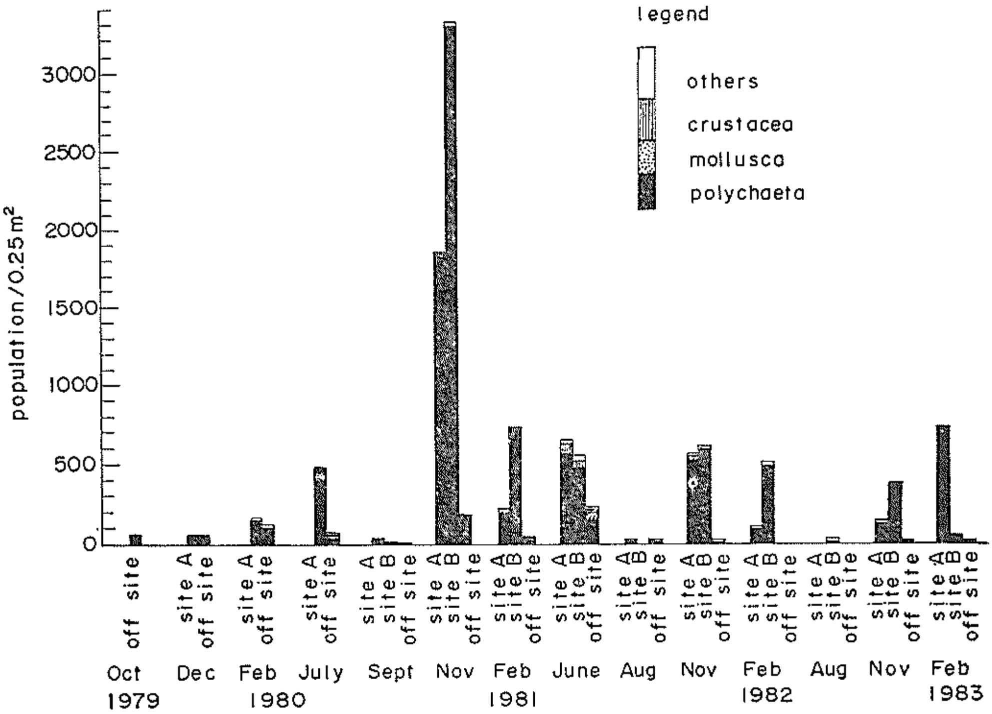

Fig. 9 Seasonal Variation of Benthos' Population inside and outside the Capping Sites

However, in the season from autumn to winter, the number of the benthos inside the treatment sites obviously increases and exceeds that of the outside.

The obvious sensitivity of the sediment treatment to benthos as shown in this observation is quite courageous for the development of new criterion, and the development of the new prediction model is required for this reason.

3.2 Assumptions

The seawater and related environment are described in Fig. 10. The seawater quality is affected by the process as the external load, the release from the bottom sediment, the internal production by marine organics, biological activities, the seawater circulation, and the seawater exchange with the outer seas. Among these processes, the biological activities of zooplankton, benthos, periphyton, fish, etc. are neglected in the previous model. However, the contribution of these activities to the nutrient cycle in the seawater and the sediment is not always negligibly small, especially in the period when the temperature rises and all biological reactions become active. Organic substances in the seawater and the sediment are decomposed by the bacteria. The respiration by phytoplankton, zooplankton, benthos and fish, the extracellular secretion by phytoplankton, the death, and feeding and excretion by sea animals are all important processes in the marine nutrient cycle. The new model is developed from this standpoint.

The following items were assumed in configuring the model.

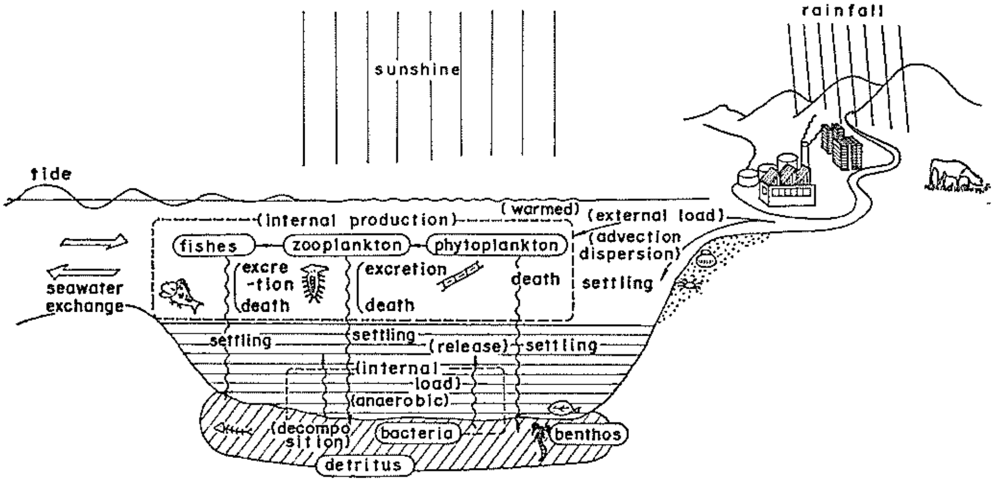

Fig. 10 Natural Ecosystems

i) the new model is built on the basis of the previous nutrient cycle model.

ii) the nutrient cycle between seawater and sediment is treated in the same system by assembling two models of the seawater system and the sediment system.

iii) the computational area is horizontally homogeneous but vertically stratified; with eleven layers in the seawater and seven layers in the sediment.

iv) compartments of the model are phytoplankton, zooplankton, oyster, detritus, dissolved organic phosphorus, inorganic phosphrus.

v) the nutrient cycle processes are growth, secretion, feeding, excretion, decomposition, respiration, death, and fish catching as biological processes, and advection, dispersion, settling, external load and release as non-biological processes.

vi) the effect of the sediment treatment on the seawater is estimated by the cut-off rate of release and the reduction of the DO uptake rate due to the decrease of T–P in the sediment.

vii) the effect of the sediment treatment on the benthos is estimated by the reduction of the death rate of benthos due to the increase of sedimental median diameter.

3.3 Formulation of basic equations

Based on the above assumptions, the new nutrient cycle model can be formed. Figure 11 shows the mutual relationship between each compartment.

For convenience, the basic equations to the seawater system are explained in section different to that of the sediment system.

(1) Seawater system

$$\frac{\partial \cdot IP \cdot h}{\partial t} = - \text{(photosynthesis)} + \text{(decomposition of DOP)}$$
$$+ \text{(decomposition of detritus)}$$
$$+ \text{(excretion by zooplankton)}$$
$$+ \text{(excretion by oyster)}$$
$$+ \text{(excretion by benthos)}$$

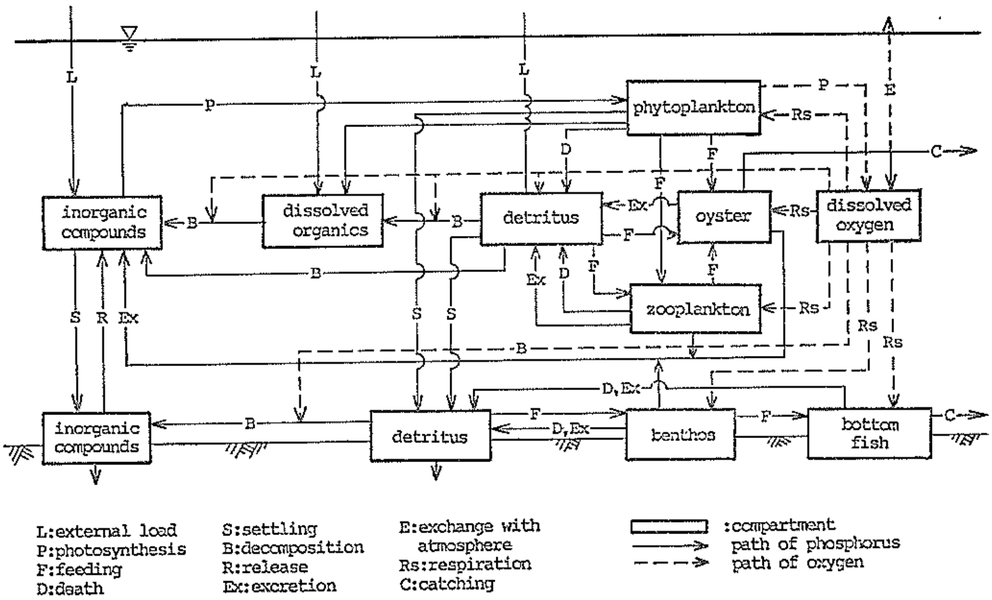

Fig. 11 The Developed Nutrient Cycle Model

$+$ (excretion by fish) $+$ (release)
$+$ (external load) $+$ (vertical dispersion)
$+$ (respiration by phytoplankton)
$+$ (settling) $+$ (vertical advection)
$+$ (horizontal advection)

$$
\begin{aligned}
&= -B_1 \cdot P \cdot h + B_{11} \cdot DOP \cdot Z + B_{13} \cdot D \cdot h + B_8 \cdot Z \cdot h \\
&\quad + \underline{B_{29}} + \underline{B_{16} \cdot B} + \underline{B_{21} \cdot F} + \underline{B_{26}} + \underline{RIN_{IP}} \\
&\quad + \underline{K_z (IP_{n-1} - 2 \cdot IP_n + IP_{n+1})/h} + B_4 \cdot P \cdot h - \underline{B_5 \cdot (IP_n - IP_{n-1})} \\
&\quad + \underline{QZ_n \cdot IP^{*1} - QZ_{n-1} \cdot IP^{*2}} + \underline{(Q_{IN_n} \cdot AK \cdot IP - Q_{OUT_n} \cdot IP)} \qquad (11)
\end{aligned}
$$

for PO_4–P (IP).

$\frac{\partial \cdot D \cdot h}{\partial t} = -$ (decomposition) $-$ (dissolution) $-$ (settling)
$+$ (death of phytoplankton)
$+$ (death of zooplankton)
$+$ (excretion by zooplankton)
$-$ (feeding by zooplankton)
$+$ (excretion by oyster)
$-$ (feeding by oyster) $+$ (vertical dispertion)
$+$ (vertical advection) $+$ (horizontal advection)

$$
\begin{aligned}
&= -B_{13} \cdot D \cdot h - K_D \cdot B_{13} \cdot D \cdot h \cdot - \underline{B_{12} \cdot (D_n - D_{n-1})} + B_2 \cdot P \cdot h \\
&\quad + B_{10} \cdot Z \cdot h + B_7 \cdot Z \cdot h - \frac{D}{P+D} B_6 \cdot Z \cdot h + \underline{B_{28}} \\
&\quad - \underline{\frac{D}{P+Z+D} \cdot B_{27}} + \underline{RIN_D} + \underline{K_Z \cdot (D_{n-1} - 2 \cdot D_n + D_{n+1})/h} \\
&\quad + \underline{QZ_n \cdot D^{*1} - QZ_{n-1} \cdot D^{*2}} + \underline{(Q_{IN_n} \cdot AK \cdot D - Q_{OUT_n} \cdot D)} \qquad (12)
\end{aligned}
$$

for detritus (D).

$$\frac{\partial \cdot DOP \cdot h}{\partial t} = \text{(secretion by phytoplankton)}$$
$$+ \text{(dissolution of detritus)} - \text{(dissolution)}$$
$$+ \text{(external load)} + \text{(vertical dispersion)}$$
$$+ \text{(vertical advection)} + \text{(horizontal advection)}$$
$$= B_3 P \cdot h + K_D \cdot B_{13} \cdot D \cdot h - B_{11} \cdot DOP \cdot h + \underline{RIN_{DOP}}$$
$$+ \underline{K_Z \cdot (DOP_{n-1} - 2 \cdot DOP_n - DOP_{n+1})/h}$$
$$+ \underline{QZ_n \cdot DOP^{*1}} - \underline{QZ_{n-1} \cdot DOP^{*2}} + \underline{(Q_{IN_n} \cdot AK \cdot DOP - Q_{OUT_n} \cdot DOP)} \quad (13)$$

for dissolved organic phosphorus (DOP).

$$\frac{\partial \cdot DO \cdot h}{\partial t} = \text{(photosynthesis)} - \text{(respiration by phytoplankton)}$$
$$- \text{(respiration by zooplankton)}$$
$$- \text{(respiration by oyster)} - \text{(respiration by benthos)}$$
$$- \text{(respiration by fish)} - \text{(uptake by DOP decomposition)}$$
$$- \text{(uptake by detritus decomposition)}$$
$$+ \text{(reaeration)} - \text{(uptake by the sediment)}$$
$$+ \text{(vertical dispersion)} + \text{(vertical advection)}$$
$$= K_{P1} \cdot B_1 \cdot P \cdot h - K_{P1} \cdot B_4 \cdot P \cdot h - B_9 \cdot Z \cdot h - \underline{B_{31}}$$
$$- \underline{B_{17} \cdot B} - \underline{B_{23} \cdot F} - K_{OP1} \cdot B_{11} \cdot DOP \cdot h$$
$$- K_{D1} \cdot B_{13} \cdot D \cdot h + \underline{BAKI \cdot (HOWA - DO_1)} - \underline{B_{25}}$$
$$+ \underline{K_Z \cdot (DO_{n-1} - 2 \cdot DO_{n+1} + DO_{n+1})/h}$$
$$+ \underline{QZ_n \cdot DO^{*1} - QZ_{n-1} \cdot DO^{*2}} + \underline{(Q_{IN_n} \cdot AK \cdot DO - Q_{OUT_n} \cdot DO)} \quad (14)$$

for DO.

$$\frac{\partial \cdot P \cdot h}{\partial t} = \text{(photosynthesis)} - \text{(death)} - \text{(secretion)}$$
$$- \text{(respiration)} - \text{(grazing by zooplankton)}$$
$$- \text{(feeding by oyster)} + \text{(vertical dispersion)}$$
$$+ \text{(vertical advection)} + \text{(horizontal advection)}$$
$$= B_1 \cdot P \cdot h - B_2 \cdot P \cdot h - B_3 \cdot h - B_4 \cdot P \cdot h$$
$$\frac{P}{P+D} \cdot B_6 \cdot Z \cdot h - \underline{\frac{P}{P+D+Z} \cdot B_{27}}$$
$$+ \underline{K_Z \cdot (P_{n-1} - 2P_n + P_{n+1})/h}$$
$$+ \underline{QZ_n \cdot P^{*1} - QZ_{n-1} \cdot P^{*2}} + \underline{(Q_{IN_n} \cdot AK \cdot P - Q_{OUT_n} \cdot P)} \quad (15)$$

for phytoplankton (P).

$$\frac{\partial \cdot Z \cdot h}{\partial t} = \text{(grazing of phytoplankton)} + \text{(feeding of detritus)}$$
$$- \text{(urination)} - \text{(excretion of faeces)}$$
$$- \text{(death)} - \text{(feeding by oyster)} + \text{(vertical dispersion)}$$
$$+ \text{(vertical advection)} + \text{(horizontal advection)}$$
$$= \frac{P}{P+D} \cdot B_6 \cdot Z \cdot h + \frac{D}{P+D} \cdot B_6 \cdot Z \cdot h - B_7 \cdot Z \cdot h - B_8 \cdot Z \cdot h$$
$$- B_{10} \cdot Z \cdot h - \underline{\frac{Z}{P+D+Z} \cdot B_{27}} + \underline{K_Z (Z_{n-1} - 2 \cdot Z_n + Z_{n+1})/h}$$
$$+ \underline{QZ_n \cdot Z^{*1} - QZ_{n-1} \cdot Z^{*2}} + \underline{(Q_{IN_n} \cdot AK \cdot Z - Q_{OUT_n} \cdot Z)} \quad (16)$$

for zooplankton (Z).

where,

h	:	layer thickness
AK	:	dilution factor at open boundary
RIN_{IP}	:	effluent load of PO_4–P
RIN_P	:	effluent load of POP (particulate organic phosphorus)
RIN_{DOP}	:	effluent load of DOP (dissolved organic phosphorus)
K_Z	:	vertical dispersion coefficient
K_D	:	ratio of detritus dissolution to its decomposition
$BAKI$	:	reaeration coefficient
K_{OP1}	:	ratio of DOP/TOD
K_{D1}	:	ratio of TOD/P in detritus
$HOWA$	:	saturated DO in the 1st layer
Q_{INn}	:	horizontal inflow mass balance of seawater in the n th layer
Q_{OUT}	:	horizontal outflow mass balance of seawater in the n th layer
Q_Z	:	vertical mass balance from $n+1$ th layer to n th layer (upward positive)
QZ_{n-1}	:	vertical mass balance from n th layer to $n-1$ th layer (upward positive)
IP^{*1}	:	$IP^{*1}=IP_{n+1}$ for $QZ_n \geqq 0$, $IP^{*1}=IP_n$ for $QZ_n<0$
IP^{*2}	:	$IP^{*2}=IP_n$ for $QZ_{n-1} \geqq 0$, $IP^{*2}=IP_{n-1}$ for $QZ_{n-1}<0$

(The similar manner is available for other compartments.)

The underlined terms in the above equations imply that the treatment of terms differ with the layer: the external loads are taken into account only in the 1st layer, oysters are treated at the layers from the 1st to 5th, and the excretion by benthos and fish are treated only in the lowest layer.

The vertical distribution, the vertical advection, and the horizontal advection are treated in whole layers.

(2) Sediment system

$$\frac{\partial \cdot IP_B \cdot h}{\partial t} = \text{(supply by settling)} + \text{(decomposition of detritus)} - \text{(release)} - \text{(outflow)}$$
$$= B_{12} \cdot IP + \text{the seabed sediment model} \qquad (17)$$

for PO_4–P in the sediment (IP_B).

$$\frac{\partial \cdot D_B \cdot h}{\partial t} = \text{(supply by settling)} - \text{(feeding by benthos)} + \text{(excretion by benthos)} + \text{(death of benthos)} + \text{(excretion by fish)} + \text{(death of fish)} - \text{(decomposition)} + \text{(bioturbance)} - \text{(outflow)}$$
$$= B_{12} \cdot D - B_{14} \cdot D_B + B_{15} \cdot B + B_{18} \cdot B + B_{20} \cdot F + B_{22} \cdot F + \text{the seabed sediment model} \qquad (18)$$

for detritus in the sediment (D_B).

$$\frac{\partial B}{\partial t} = \text{(feeding of detritus)} - \text{(excretion of faeces)} - \text{(urination)} - \text{(death)} - \text{(feeding by fish)}$$
$$= B_{14} \cdot B - B_{15} \cdot B - B_{16} \cdot B - B_{18} \cdot B - B_{19} \cdot F \qquad (19)$$

for benthos (B).

$$\frac{\partial F}{\partial t} = \text{(feeding of benthos)} - \text{(excretion of faeces)} - \text{(urination)} - \text{(death)} - \text{(catching)}$$

$$=B_{19}\cdot F-B_{20}\cdot F-B_{21}\cdot F-B_{22}\cdot F-B_{24} \tag{20}$$

for bottom fish (F).

The seabed sediment model in equations (17) and (18) is identical to the model stated in **2.4(2)**.

4. Formulation of Each Process and Fitting of Parameters

4.1 Ecological process

Parameters from B_1 to B_{31} appeared in equations (11) to (20) and are mostly determined on the basis of previous investigations obtained by many researchers. The function and the value of these parameters are determined for the application to Kure Bay, as listed in Table 4.

4.2 Physical process

(1) Light

Solar radiation plays an important role in the phytoplankton growth. It would therefore be desirable to formulate a scheme for the incident solar radiation that incorporated day-to-day variations. However, for the present model, daily averaged sunlight at the sea surface (I_0) is used by fitting observed data to a smooth average curve for the seasonal trend.

The illumination at an arbitrary layer (I_i) is estimated by the following equation:

$$I_i=I_0 \exp(-k\cdot z) \tag{21}$$

where

k: extinction coefficient (1/m)

z: vertical distance from the sea surface (m)

The extinction coefficient (k) is estimated by[12]

$$\log_{10} k=1.439\times\frac{1}{Tr}-0.885 \tag{22}$$

where

Tr: transparency of the seawater

The transparency is related with the O–P in the surface layer in Kure Bay as shown in Fig. 12, and formulated into the following equation:

$$Tr=0.764\times(\text{O-P})^{-0.473} \tag{23}$$

(2) Seawater temperature and salinity

Seawater temperature is one of the most influential forces that control physical and ecological processes.

The vertical distribution of salinity and temperature related with the stratification of the seawater and the vertical dispersion of substances. In the same manner as for surface illumination, the daily averaged temperature and salinity are formulated into a smooth average curve for the seasonal trends.

(3) Vertical dispersion

The vertical dispersion is generally promoted in the mixing period during winter,

Table 4 Parameters, Functions, and Constants of the Nutrient Cycle Model

Parameter	Function	Value	Reference
(Phytoplankton)			
B_1: growth rate (1/day)	$B_1=\mu_{max}\cdot f(I)\cdot f(T)\cdot f(N)$ $f(I)=\frac{1}{I_{opt}}\cdot\exp\left(1-\frac{1}{I_{opt}}\right)$ $f(T)=\exp\{0.053(T-18)\}$ $f(N)=\frac{IP}{K_{IP}+IP}$	$\mu_{max}=1.4(0.4\sim2.1)$ $I_{opt}=1.7\times10^4(10^4\sim2.7\times10^4)$ I_{opt}: optimum illumination (lux) T: temperature (℃) K_{IP}: 0.015	ref.[3),5)] Ryther, J. H.[4)] (1956) 3rd District Port Construction Bureau
B_2: mortality (1/day)		0.040 (0.010∼0.10)	ref.[6)~8)]
B_3: extracellar secretion		0.130 (0.127∼0.135)	Watt (1966)[9)]
B_4: respiration rate (1/day)	$B_4=0.03\exp(0.052T)$	0.025	ref.[10)]
B_5: settling rate (m/day)	not considered		ref.[10)] Nakata (1985)[11)]
(Zooplankton)			
B_6: grazing rate (1/day)	$B_6=V_{max}\cdot\exp\{K_1(T-20)\}$ $\times[1-\exp\{\lambda(P^*-P-D)\}]$ $\times f(DO)$ $f(DO)=\frac{DO-1}{DO-1+1}$	V_{max}: maximum grazing rate at 20℃ (1/day) $V_{max}=1.4$ (1.5∼2.5) K_1: temperature factor (=0.0693) λ: constant (=8.2) $(mg/l)^{-1}$ P^*: threshold=0.0020 (0.0012∼0.0024) (mg/l)	ref.[10)] Nakata (1985)[11)] Adams & Steel[13)] (1966) Parsons & Lebrasseur[14)] (1970)
B_7: excretion of faeces(1/day)	$B_7=(1-\alpha)\cdot B_6$	α: assimilation efficiency =0.6 (0.5∼0.6)	ref.[15)]
B_8: excretion of urine (1/day)	$B_9=(\alpha-\gamma)\cdot B_8$	γ: growth efficiency=0.21	ref.[15)]
B_9: respiration rate (1/day)	$B_9=R_{max}\cdot\exp\{K_1(T-20)\}$	R_{max}: maximum respiration rate (mgO_2/mg·P/day) =2.973 K_1: temperature factor =0.0693	Ikeda (1977)[15)]
B_{10}: mortality (1/day)	$(1-B_{30})^{30}=0.5$	$B_{30}=0.02$	ref.[10)]
(Dissolved organics)			

Parameter	Function	Value	Reference
B_{11}: decomposition rate (1/day)	$B_{11}=B_{max}\cdot\exp(K_1\cdot T)\times\frac{DO}{DO_0+DO}$	B_{max}: decomposition rate (1/day)=0.005 K_1: temperature factor (1/℃)=0.0693 DO_0: constant (mg/l)=0.25	ref.[10]
(Detritus)			
B_{12}: settling rate of I-P (m/day)		0.036	Shimizu (1985)[17]
B_{13}: decomposition rate (1/day)	$B_{13}=B_{max}\cdot\exp(K_1\cdot T)\times\frac{DO}{DO_1+DO}$	B_{max}: decomposition rate at 0℃ (1/day)=0.005 K_1: temperature factor (mg/l)=0.07 DO_1: constant (mg/l)=0.1	ref.[10]
(Benthos)			
B_{14}: feeding rate (1/day)	$B_{14}=G_{max}\cdot f_1(T)\cdot f_2(O\text{-}P)$ $f_1(T)=\exp\{K_1(T-25)\}$ $f_2(O\text{-}P)=\frac{OP_1-0.55}{OP_1-0.55+K_2}$	G_{max}: feeding rate (1/day) =7.9 (7.9~9.87) K_1: temperature factor (1/℃)=0.0785 OP_1: O-P content in the surface layer of the sediment (mg·P/g·dry) K_2: constant (mg/l)=0.30	Tamai (1982)[20] Yokoyama (1982)
B_{15}: excretion of faeces(1/day)	$B_{15}=B_{14}(1-\alpha)$	α: assimilation efficiency =0.50	Kurihara[21] (1986)
B_{16}: excretion of urine (1/day)	$B_{16}=B_{14}(\alpha-\gamma)$	γ: growth efficiency=0.20	Yamamoto[22] (1972)
B_{17}: respiration rate (mgO_2/mg·P/day)	$B_{17}=3.86\exp\{0.0693(T-15)\}$		Ueno (1982)[23]
B_{18}: mortality (1/day)	$(1-D)^{182.5}=0.5$ D: mortality (1/day) $B_{18}=\max[f_1(DO), f_2(M)]$ (1/day) DO: DO in the bottom layer $f_2(M)=\begin{cases}0.0038 & (M\geqq1.7)\\ -0.02525M+0.04673 & (M<1.7)\end{cases}$	$D=0.0038$	

Parameter	Function	Value	Reference
	M: median diameter of the sediment $f_1(DO)=\begin{cases} 0.0038 & (3.4 \leqq DO) \\ -0.3646 \cdot DO+1.2434 & (1.6 \leqq DO \leqq 3.4) \\ -0.4857 \cdot DO+1.4371 & (0.9 \leqq DO \leqq 1.6) \\ 1.0 & (DO \leqq 0.9) \end{cases}$		
(Bottom fish)			
B_{19}: feeding rate (1/day)	$B_{19}=R_{max} \cdot f_1(T) \cdot f_2(B) \cdot f_3(DO)$ $f_1(T)=\exp\{0.0693(T-27)\}$ $f_2(B)=\begin{cases} 1 & \text{for } B/F \geqq 10 \\ B/F/10 & \text{for } B/F<10 \end{cases}$ $f_3(DO)=\begin{cases} 1 & \text{for } DO \geqq 4 \\ 0.25 \cdot DO & \text{for } DO<4 \end{cases}$ B : standing crop of benthos F : standing crop of fish	R_{max}: maximum feeding rate (1/day)=0.195	Hatanaka[24] (1977) Ibrev (1979)
B_{20}: excretion of faeces (1/day)	$B_{20}=B_{19}(1-\alpha)$	α: assimilation efficiency =0.882	
B_{21}: excretion of urine (1/day)	$B_{21}=B_{10}(\alpha-\gamma)$	γ: food conversion efficiency =0.21	Kawamoto[26] (1966)
B_{22}: mortality (1/day)	$(1-B_{22})^{365}=0.59$	$B_{22}=0.0014$	ref.[27]
B_{23}: respiration rate ($gO_2/g \cdot P$/day)	$B_{23}=1.47\exp\{0.0693(T-25)\}$		Kawamoto[26] (1966)
B_{24}: catching rate	$(1-B_{24})^{365}=0.657$	$B_{24}=0.0012$	Kawamoto (1966)[26] ref.[27]
(Sediment)			
B_{25}: DO uptake rate (mgO_2/m^2/day)	$B_{25}=D_{max} \cdot \exp\{K_1(T-18)\}(T\text{-}P)^{K_2}$	D_{max}: DO uptake at 18℃ (mgO_2/m^2/day)=365 K_1: temperature factor	3rd District Port Construction Bureau

Parameter	Function	Value	Reference
		=0.034 K_2: constant=0.299 T-P: T-P content in the sediment (mg·P/g·dry)	
B_{26}: PO_4-P release rate (mg/m²/day)			
(Oyester)			
B_{27}: feeding rate (kg·P/day)		14.83～221.84	seasonal variation
B_{28}: excretion of faeces (kg·P/day)		2.69～155.45	seasonal variation
B_{29}: excretion of urine (kg·P/day)		8.20～ 58.82	seasonal variation
B_{30}: catching (kg·P/day)		0～ 37.42	seasonal variation
B_{31}: respiration (kg·P/day)	$B_{31}=(TOD/P)\times B_{29}$	TOD/P=146.6	

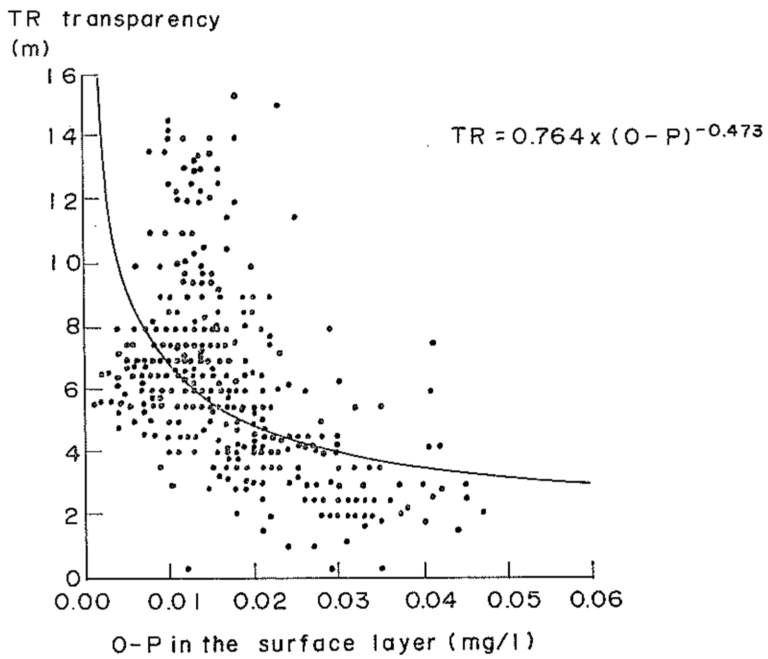

Fig. 12 Relation between O-P in the Surface Layer and Transparency

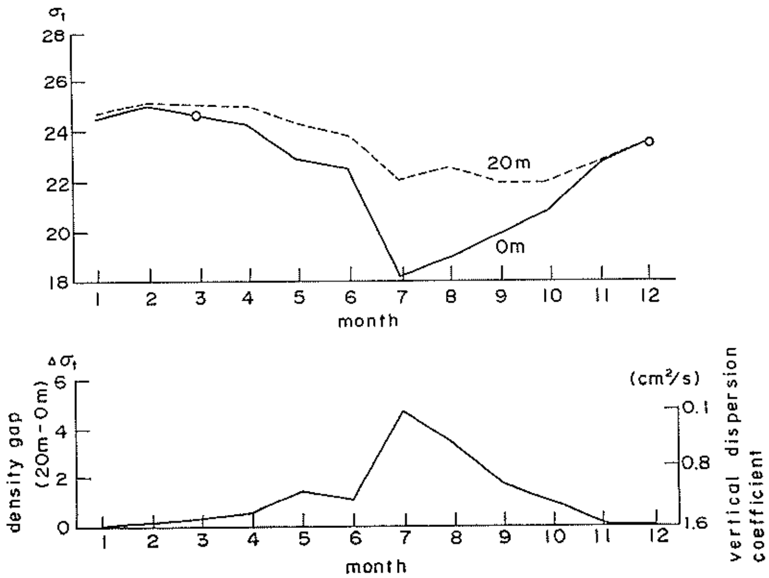

Fig. 13 Seasonal Trend of Seawater Density at Surface and That of Vertical Dispersion Coefficient

and weakened in summer. The seasonal trend of the seawater density gap at the depth between the sea surface and the bottom in Kure Bay is greater in summer and less in winter, as shown in Fig. 13. The vertical dispersion is related with the density gap, and assumed to vary in reverse proportion to the gap. Consequently, the value of the vertical dispersion coefficient varies from 1.6 cm^2/s in December to 0.1 cm^2/s in July.

5. Calibration of the Model

5.1 Input data

(1) Computational area

The newly developed model is applied to Kure Bay. The computational area is 4800 ha and adjacent to the inner bay in the north and Hayase Straits in the south.

The present model is horizontally homogeneous, e.g., uni-segment, and vertically divided into eleven layers in the seawater system and seven layers in the sediment system as shown in Fig. 14. The layer thickness in the seawater is 2 m each. However, in the sediment, the layer thickness varies to increase correspondingly with the depth.

(2) Tidal circulation and exchange

The interaction of the local tides, river flows, winds, and geography affects the dynamics of the ecological systems in many bays. However, in the uni-segment model, the inflow and the outflow to the system and the vertical mass transport of seawater have significant implication. These values are determined, as shown in Fig. 15, by the simulation results, which have already been obtained on the previous investigation as stated in **2.5(1)**.

(3) External loads of PO_4–P, dissolved O–P and detritus

The external loads of PO_4–P, dissolved O–P and detritus are respectively summed up to those within the computational area. Consequently, these values are estimated as:

the external load of PO_4–P (RIN_{IP}) 0.129 t/day

the external load of dissolved O–P (RIN_{OP}) 0.039 t/day

the external load of detritus (RIN_{D}) 0.039 t/day

These loads are given to the surface layer of the seawater in the model.

(4) Target

The target of the phosphorus to the present simulation is determned on the basis of the observation data for several years in Kure Bay. PO_4–P, DO, total phosphorus (T–P) and chlorophyl a (which is contained only in the phytoplankton) are determined by averages of the data obtained at 2 m and 20 m below the surface from 1983 to 1986. The phosphorus in the phytoplankton is estimated by multiplying the phosphorus-to-chlorophyl a ratio (=1.8 mg-P/mg- chl-a) into chlorophyl a. The phosphorus in the zooplankton is estimated by multiplying dry-weight/wet-weight ratio (=0.15) and phosphorus/dry-weight ratio (=0.006) into the dry-weight of zooplankton. In the same manner, the phosphorus in the benthos is estimated by

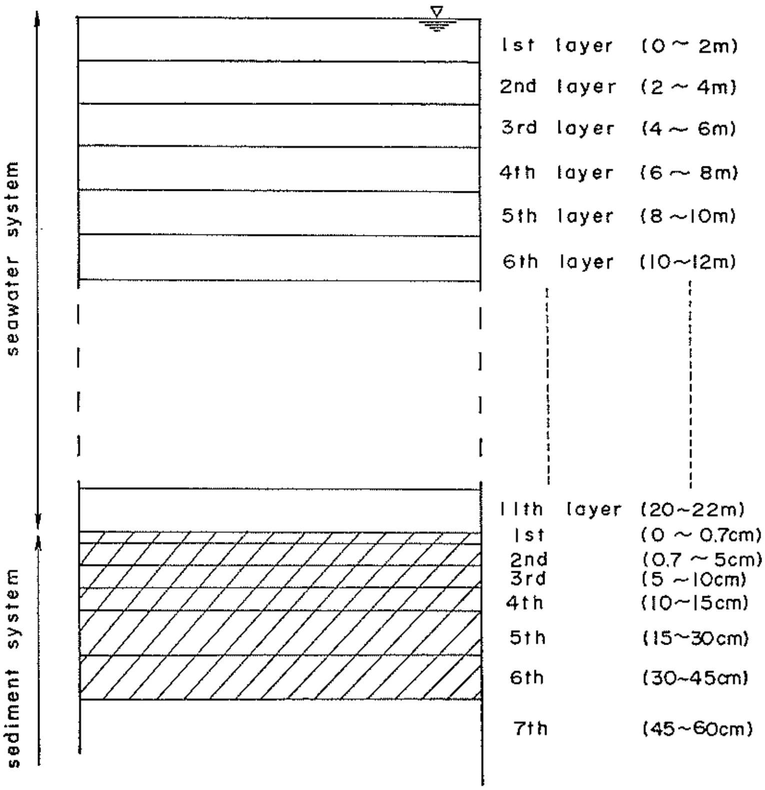

Fig. 14 Vertical Partition of Seawater and Sediment Systems

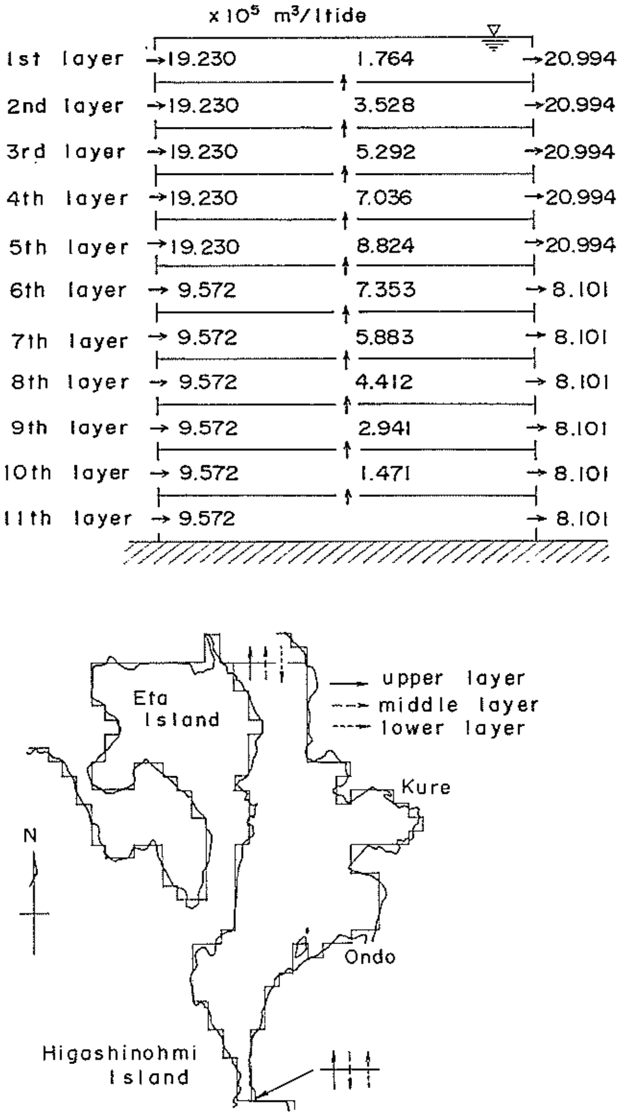

Fig. 15 Seawater Mass Balance among Each Layer

multiplying the dry-weight/wet-weight ratio of *prionospio pinnata* (=0.18) and phosphorus/dry-weight ratio (=0.0084) into macrobenthos. Some of the above targets are shown in Fig. 15 to Fig. 21.

(5) Initial values

Initial values of the seawater quality and the sediment are given as listed in Table 5. The initial values of PO_4–P, DO, phytoplankton, zooplankton and benthos are determined on the basis of the data obtained in winter observation. Initial values of O–P, I–P, and interstitial PO_4–P in the sediment are obtained from the

Table 5 Initial Values

Item	Value							Based on
(Seawater)								
PO_4-P	0.02 mg/l from 1st to 11th layer							average with respect to total depth in winter
detritus	0.007 mg/l from 1st to 11th layer							detritus: phytoplankton=1 : 1
DOP	0.004 mg/l from 1st to 11th layer							DOP=TP−PO_4-P−detritus−phytoplankton−zooplankton
DO	9.0 mg/l from 1st to 11th layer							average with respect to total depth in winter
phytoplankton	0.007 mg/l from 1st to 5th layer							observed value in the uppper layer in winter
zooplankton	0.002 mg/l from 1st to 11th layer							observed value in winter
(Sediment)								
P in benthos	30 mg/m^2 in 1st layer							observed value in winter
P in bottom fish	3.57 mg/m^2 in 1st layer							catching amount of bottom fish/catching efficiency/10
	1st layer	2nd	3rd	4th	5th	6th	7th	simulation results by the sediment model
O-P in the sediment (mg/g)	0.57	0.56	0.55	0.55	0.43	0.31	0.31	
I-P in the sediment (mg/g)	0.28	0.28	0.26	0.26	0.26	0.26	0.24	
interstitial PO_4-P (mg/l)	0.03	1.17	0.91	1.00	1.09	0.91	0.79	
time increment	1 hour							calculation stability
calculation time	for five years							repetation time needed to reach a certain trend of seasonal variation

result of the seabed sediment simulation described in **2.4(2)**.

5.2 Results

By using the developed model and the obtained data, the simulation was carried out with a time increment (Δt) of 1 hour. Most of simulated variables are found to have their own seasonal trends over five years. Figures 16 to 21 show the simulation results with the corresponding observed values, in the surface layer and the bottom layer, except for Fig. 21. According to these results, the calculated PO_4–P generally agrees well with the observed values, especially those in the bottom layer through the year, but from September to December, half or less in the surface layer. Contrary to PO_4–P, the calculated O–P values are about twice of the observed values. The calculated DO generally agrees well with observed values both in the surface and the bottom and the calculated phytoplankton in the surface layer are higher than the observed values from August to February (about twice or more), and about one half in June. Some biologists may insist that the significance of the peak value of phytoplankton because this peak value, called 'spring blooming', may make a great

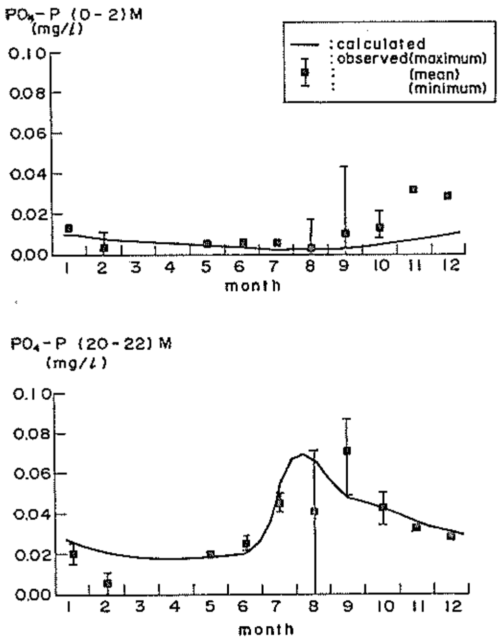

Fig. 16 Calibration of the Model on PO_4-P

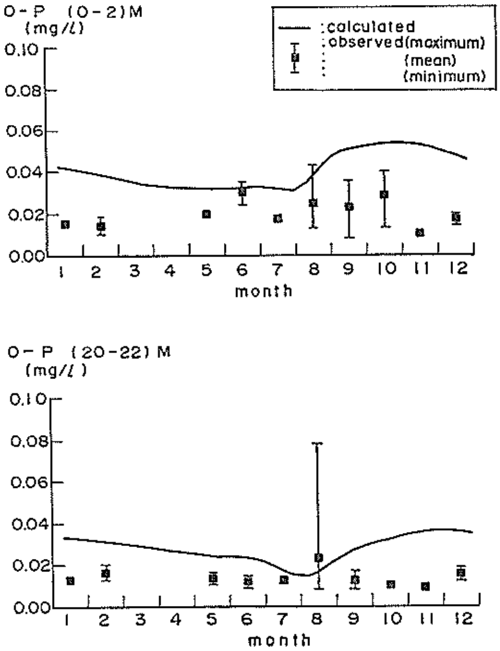

Fig. 17 Calibration of the Model on O-P

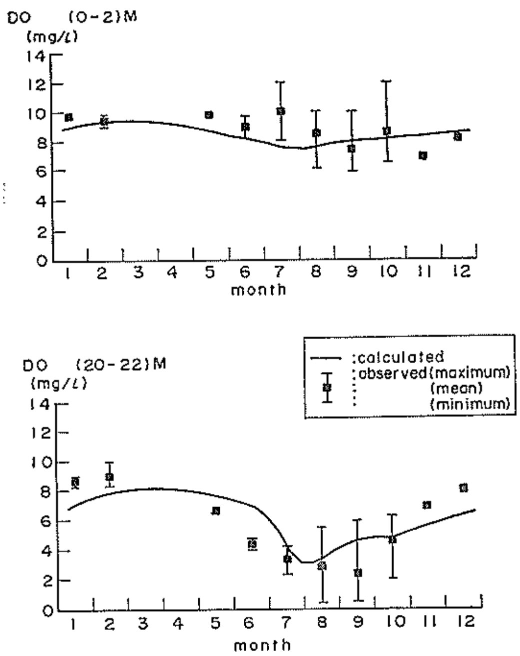

Fig. 18 Calibration of the Model on DO

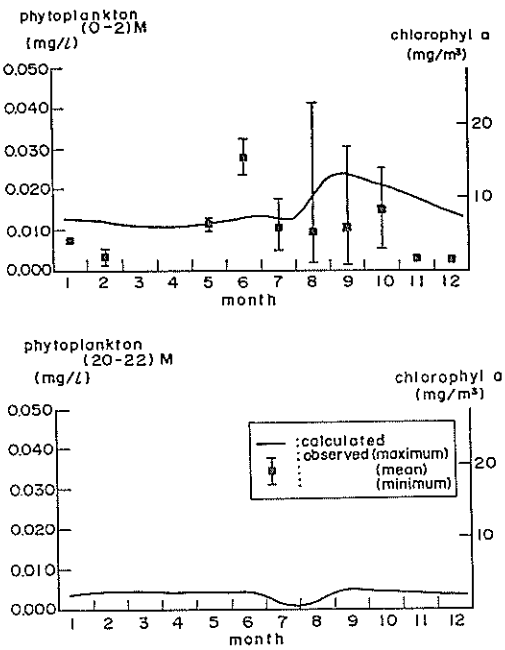

Fig. 19 Calibration of the Model on Phytoplankton

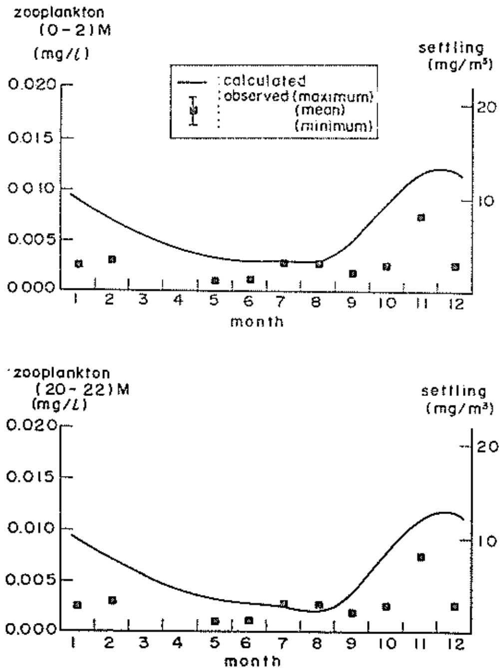

Fig. 20 Calibration of the Model on Zooplankton

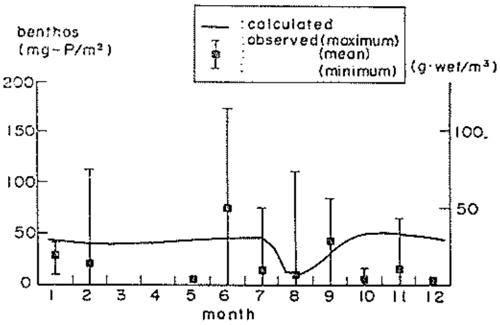

Fig. 21 Calibration of the Model on Benthos

contribution to the nutrient cycle in the bay. For this sense, the calculated phytoplankton in June is about one half of the observed one and is so small that it should be modified as to increase. For the zooplankton, the calculated values agree well with those in summer, but are almost twice of those from September to June. Calculated values for benthos in the sea bed are greater than the observed values, except for June and September and the observed values for benthos are greatest in June, and have almost the same trend as phytoplankton.

5.3 Sensitivity analysis

Of the many coefficients and parameters used to specify the rates and interactions in the developed model, only a few may be assigned numerical values with a high degree of certainty, and any of them will be more or less influential to the nutrient cycle in the whole system. This uncertainty is not avoidable if one considers the large amount of biological, spatial, and temporal variability that is characteristic of natural systems. In addition, there are numerous technical difficulties that one encounters when trying to estimate ecological processes in the laboratory or in the field. For these reasons, the choice of any one value for a coefficient may be questioned. When one tries to perform reasonable modification for the values used in the standard run, one is also careful to find out how sensitive the simulation is to those particular choices. The procedure of varying coefficients, functions, or initial conditions not only provides insight into the behaviors of the model, but into the more complex natural system as well.

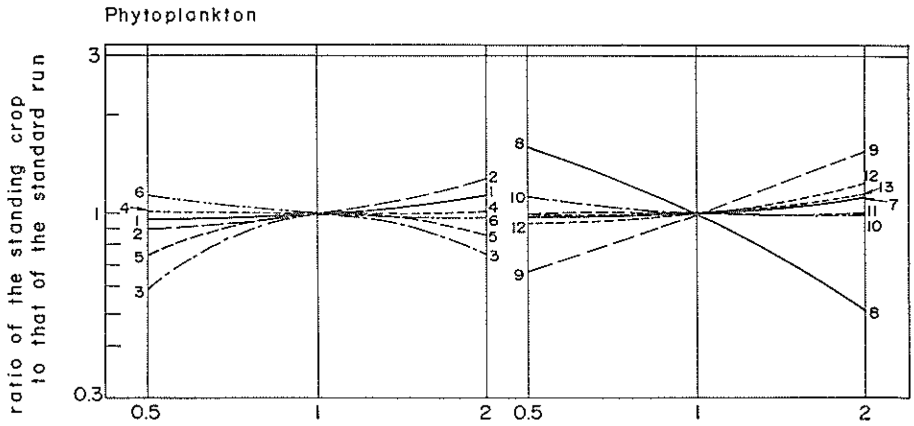

1 vertical dispersion coefficient
2 detritus settling rate
3 dilution factor
4 reaeration coefficient
5 external load
6 phytoplankton growth rate
7 PO4 -P semi-saturation constant
8 zooplankton grazing rate
9 zooplankton mortality
10 zooplankton feeding rate
11 bottom fish feeding rate
12 oyster standing crop
13 benthos mortality

Fig. 22 Sensitivity Analysis (Phytoplankton)

Thus, a series of sensitivity analyses are carried out by varying such coefficients as the vertical dispersion coefficient (K_z), the settling rate of detritus (B_{12}), the dilution factor (AK), the reaeration coefficient (BAK), the external load of PO_4–P, POP, and DOP (RIN_{IP}, RIN_P, RIN_{DOP}), the growth rate of phytoplankton (K_{IP}), the the grazing rate of zooplankton (B_6), the mortality of zooplankton (B_{10}), the feeding rate of benthos (B_{14}), the feeding rate of bottom fish (B_{19}), the standing crop of oysters, and the mortality of oysters (B_{18}).

The above coefficients are varied with the range from one half to twice to those of the standard run. The relationship between the standing crop of compartment and varied coefficients, normalized with those of the corresponding standard run, are shown for phytoplankton, zooplankton, benthos, and bottom fish in Fig. 22 to Fig. 25, respectively. From the above comparisons, the biological compartments like zooplankton, benthos, and bottom fish are seemed to be very sensitive to coefficients or parameters in the model. To conduct a successful solution for the ecological analysis, the modification of coefficients, parameters, functions, or numerical constitutions of the model should be carried out with the deep consideration of the above sensitivity. Fortunately, such intense sensitivity of the compartments gives us the encouragement for improving the biological aspects of the marine environment.

6. Concluding Remarks

A numerical ecosystem model is needed as a tool for predicting the response of natural systems to environmental improvement works of various kinds. Such

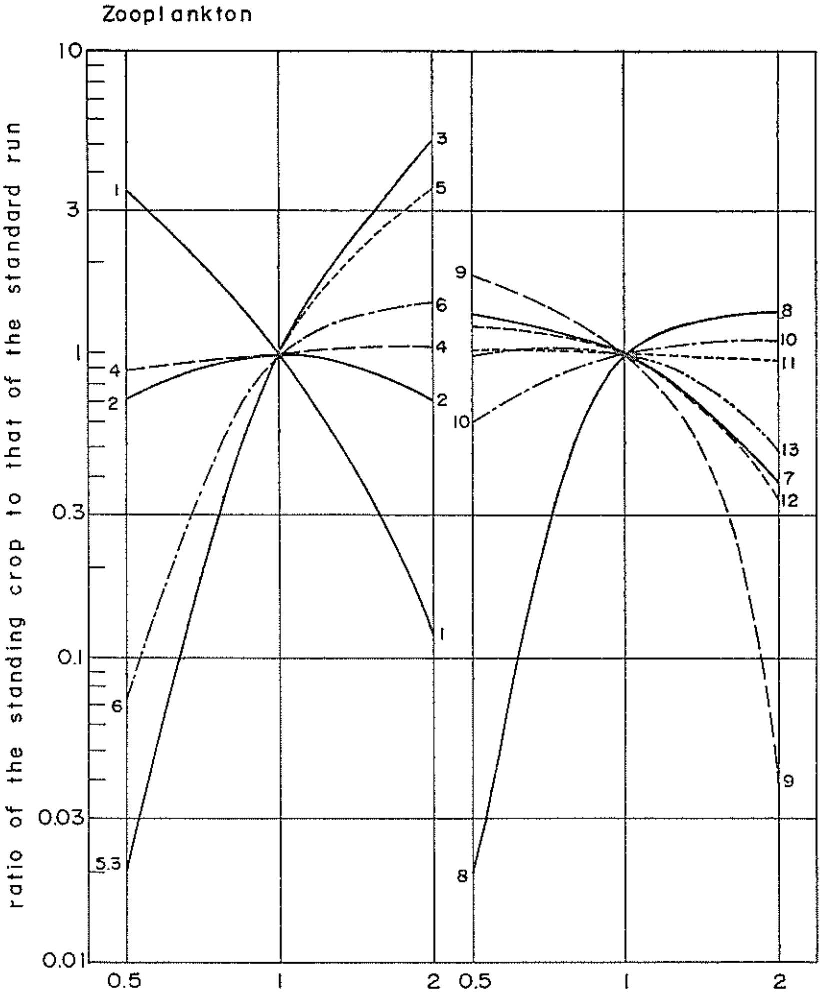

1 vertical dispersion coefficient
2 detritus settling rate
3 dilution factor
4 reaeration coefficient
5 external load
6 phytoplankton growth rate
7 PO_4-P semi-saturation constant
8 zooplankton grazing rate
9 zooplankton mortality
10 zooplankton feeding rate
11 bottom fish feeding rate
12 oyster standing crop
13 benthos mortality

Fig. 23 Sensitivity Analysis (Zooplankton)

applications may be useful, but the results yielded must be interpreted with a deep understanding of the natural systems for there are still many difficulties between model systems and real ecosystems at the present stage of development of numerical techniques. In this sense, the model developed here is only the beginning, and opens to future development. The author intends to improve the model through future investigations and to respond to the demand for a tool for the prediction of natural

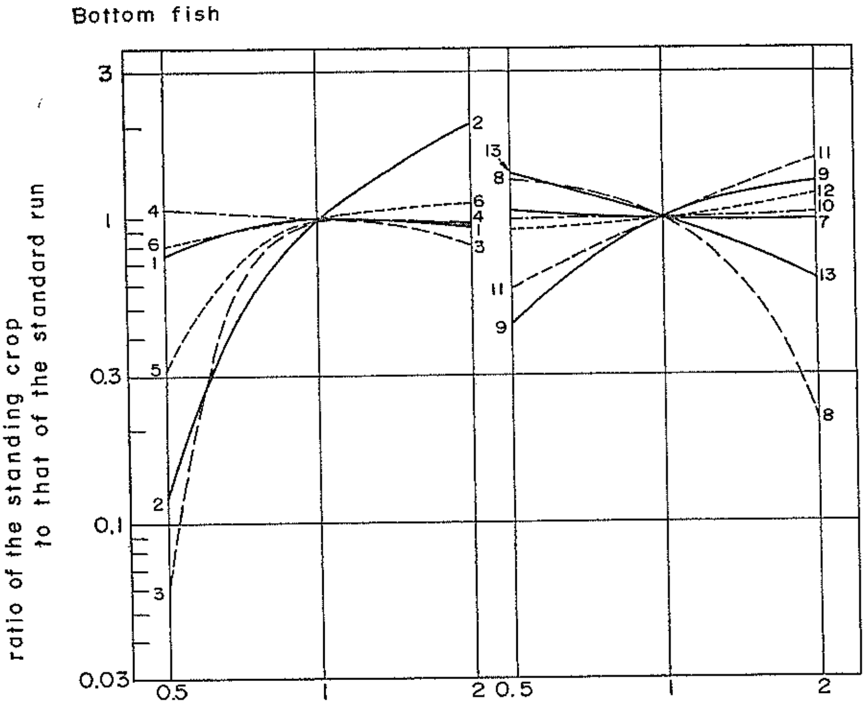

1 vertical dispersion coefficient
2 detritus settling rate
3 dilution factor
4 reaeration coefficient
5 external load
6 phytoplankton growth rate
7 PO_4-P semi-saturation constant
8 zooplankton grazing rate
9 zooplankton mortality
10 zooplankton feeding rate
11 bottom fish feeding rate
12 oyster standing crop
13 benthos mortality

Fig. 24 Sensitivity Analysis (Bottom Fish)

ecosystems.

The main items clarified in the present investigation are summarized as follows:

1. The numerical model generally plays an important role in compensating for the demerits of laboratory tests and field experiments, but the reliability of the model depends on the certainty of the data obtained by laboratory tests and field experiments.
2. Nutrient cycle models, which treat the mutual nutrient budget between inorganic and organic substances, is formulated to such a simple relation as growth and decomposition.
3. The nutrient cycle treated by only phosphorus is applied to the present investigation for the reason that phosphorus is a factor limiting the nutrient cycle in eutrophic bays.
4. The apparent improvement effect of the sea-bed treatment on seawater quality is unexpectedly small because of advection and dispersion due to seawater

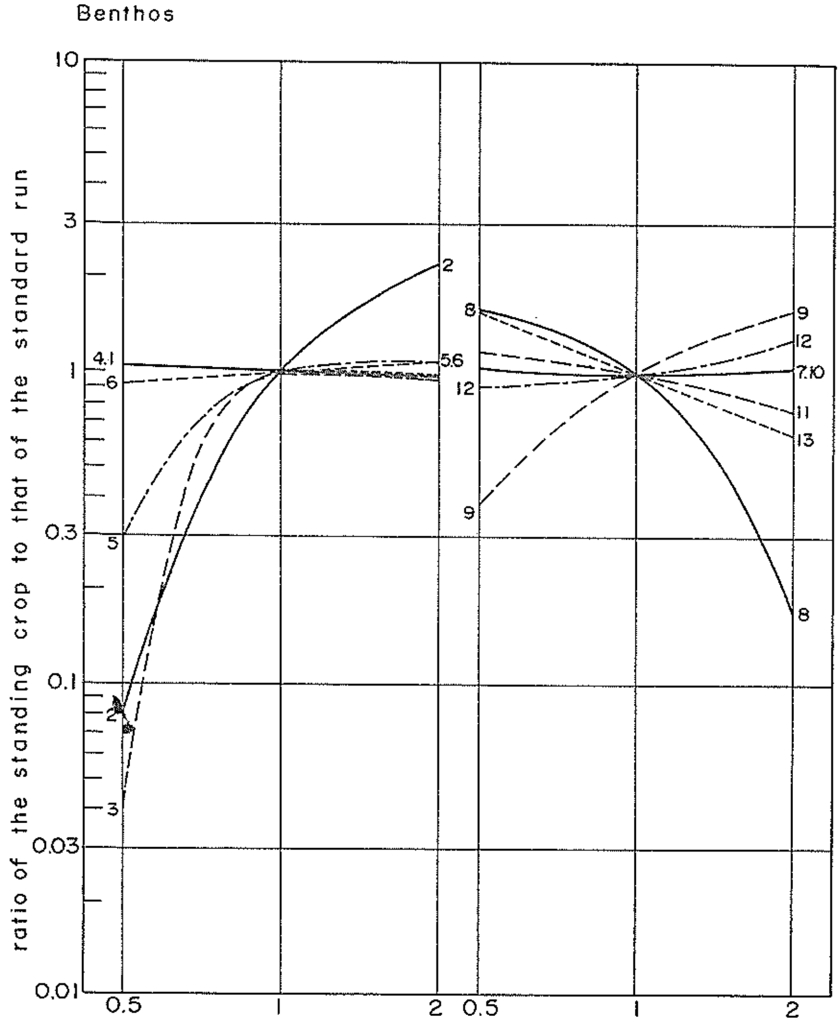

1 vertical dispersion coefficient
2 detritus settling rate
3 dilution factor
4 reaeration coefficient
5 external load
6 phytoplankton growth rate
7 PO_4-P semi-saturation constant
8 zooplankton grazing rate
9 zooplankton mortality
10 zooplankton feeding rate
11 bottom fish feeding rate
12 oyster standing crop
13 benthos mortality

Fig. 25 Sensitivity Analysis (Benthos)

circulation.

5. The release-cut-off by the capping is predicted to be very effective for the first fifteen years, but is reduced to the present rate with the elapse of time.
6. The field observation proves that the population of benthos inside the treatment sites obviously increases and exceeds that of the outside, in the season from

autumn to winter.

7. The new nutrient cycle model is built by assembling two models for the seawater and the sediment systems, which consist of compartments for phytoplankton, zooplankton, oyster, detritus, dissolved organic phosphorus, and inorganic phosphorus.
8. According to the calibration results of the model, the seasonal trend of PO_4–P, DO agrees well with the observation data, and the standing crop of phytoplankton and benthos is the agreeable value, but the phytoplankton observed around June is not well reproduced. The calculated zooplankton exceeds observed values from Descember to February.
9. The biological compartments like zooplankton, benthos, and bottom fish are very sensitive to coefficients or parameters in the model.
10. The intense sensitivity of the compartments implies the high possibility to the marine environmental improvement in biological aspects.

(Received on November 11, 1987)

Acknowledgment

This investigation was financially supported by the Second, Third, Fourth and Fifth District Port Construction Bureaus and the Environmental Protection Division of the Bureau of Ports and Harbours, Ministry of Transport. The author expresses his greatest thanks to Prof. T. Horiguchi of Tokyo Metropolitan University, Associate Prof. T. Morioka of Osaka University, Associate Prof. M. Ukita of Yamaguchi University, and Dr. H. Joh of Osaka Regional Fishery Research Laboratory, who gave him a great deal of most appropriate instruction for the performance of this investigation.

References

1) HORIE, T. and Y. HOSOKAWA: Water quality controlling factors in an eutrophic model, *Report of the Port and Harbour Research Institute,* Vol. 22, No. 3, 1983. 3, pp. 159–205 (in Japanese).

2) HORIE, T. and Y. HOSOKAWA: Mathematical model for the prediction of phosphorus release, *Report of the Port and Harbour Research Institute,* Vol. 24, No. 1, 1985. 3, pp. 43–68.

3) JOGENSEN, S. E., *et al.*: *Handbook of Environmental Data and Ecological Parameters,* International Society for Ecological Modelling, 1979.

4) RYTHER, J. H.: Photosynthesis in the ocean as a function of light intensity, *Limnological Oceanography,* 1., 1956, pp. 81–70.

5) KREMER, J. N. and S. W. NIXON: *A Coastal Marine Ecosystem,* Springer-Verlag, 1978, 217p.

6) MCKELLAR, H. N.: Metabolism and model of an estuarine bay ecosystem affected by a coastal power plant, *Ecological Modelling,* 3, 1977.

7) KISHI *et al.*: Numerical model of red-tide ecosystem, *Bulletin on Coastal Oceanography,* Vol. 22, No. 2, 1985 (in Japanese).

8) RADACH, G.: Simulation of phytoplankton dynamics and their interactions with other system components during FLEX '76, *North Sea Dynamics,* Springer-Verlag, Berline, 1987.

9) WATT, W. D.: Release of dissolved organic material from the cells of phytoplankton populations, *Proc. of Soc. London,* Ser. B., 164, 1966.

10) Association of Industrial Pollution Protection: Report on the prediction of eutrophication, 1984 (in Japanese).
11) NAKATA, K. and . TAGUCHI: Numerical investigation on the eutrophication processes in bays by using ecological-hydrodynamics model, *Bulletin of Pollution and Resource Research Institute*, 11(4), 1982, pp. 47–69 (in Japanese).
12) MUKAI, T. *et al.*: Optical properties of sea water and their seasonal variations in the coastal sea, *Japan Journal of Water Pollution Research*, Vol. 17, No. 1, 1984, pp. 11–19 (in Japanese).
13) ADAMS, J. A. and J. H. STEELE: Shipboard experiments on the feeding of *calanus finmulticus* (*Gunnerus*). *nI Some Contemporary Studies in Marine Science*, H. Barnes, Ed., Allen & Unwin, London, 1966, pp. 19–35.
14) PARSONS, J. R. *et al.*: Production studies in the Strait of Georgia. II., Secondary production under the Fraser River plume, February to May, 1967. J. Exp. Mar. Biol. Ecol., 3, 1969, pp. 39–50.
15) OHMORI and IKEDA: *Research on Zooplankton Ecology*, Kyoritsu Book Company, 1979, pp. 142–158 (in Japanese).
16) MARUMO, T.: *Marine Plankton*, Tokyo University Press, 1974 (in Japanese).
17) SHIMIZU, T., E. DATE and H. IZAWA: Settling fluxes of suspended particulate matter estimated from sediment trap catches in Hiroshima bay, *Japan Journal of Water Pollution Research*, Vol. 18, No. 5, 1985, pp. 42–51 (in Japanese).
18) SAKAMOTO, I.: Nitrogen and Phosphorus control from the viewpoint of feeding for fishery nourishment, *Nitrogen and Phosphorus Control from the viewpoint of Fishery in Closed Bay*, Kouseisha Kouseikaku Book Company, 1986, pp. 96–133 (in Japanese).
19) KUSUNOKI and KIMURA: Relation between growth of oyster and the amount of food, *Report of Hiroshima Prefectural Fishery Research Laboratory*, Vol. 13, 1983 (in Japanese).
20) TAMAI, K.: Seasonal trend and growth of *paraprionospio* sp. *A* in Osaka bay, *Journal of Japan Fishery*, 48(3), 1982, pp. 401–408 (in Japanese).
21) KURIHARA, Y.: *Marsh is Living*, Iwanami Book Company, 1986, 219p. (in Japanese).
22) YAMAMOTO, G. and R. KITAMORI: Production of benthos in Sendai Bay (Series 5), The 46th Era of Showa Special Research Project of Ministry of Education, 1972, pp. 39–48 (in Japanese).
23) UENO, S.: Ecological study on *polychaeta* and *rotatoria* in the organic pollution area of Suruga Bay, Thesis of Tokai University, 1983 (in Japanese).
24) HATANAKA, M.: Experimental estimation of substance conversion efficiency in fish stage, *Marine Ecology and Their Measurement*, Japan Society of Fishery, Kouseisha Kouseikaku, 1977, pp. 52–66 (in Japanese).
25) Yamaguchi, Fukuoka and Oh-ita Prefectures: *Management Regularization of Fishery in Coastal Area*, 1986 (in Japanese).
26) KAWAMOTO, N.: Physiology and ecology of fishes, Kouseisha Kouseikaku, 1966, 374p. (in Japanese).
27) Hiroshima Statistics nd aIn Information Office of Chugoku and Shikoku Agricultural Management Bureaus: *Annual Report of Agricultural, Forest and Fishery Statistics in Hiroshima Prefecture*, 1985 (in Japanese).
28) Resource Investigation Group of Science and Technology Agency: *Japan Standard Table of Food Content*, 1985 (in Japanese).
29) Japan Meteological Agency: *Japan Weather Chart —Series 2—, 1982*, 1982 (in Japanese).
30) Hiroshima Prefectural Fishery Research Laboratory: *Report of Hiroshima Prefectural Fishery Research Laboratory*, 1982–85 (in Japanese).
31) Tokai University Press: *Marine Physics I*, 1981, 373p. (in Japanese).